UNIVERSIDADE FEDERAL DE MINAS GERAIS
PROGRAMA DE PÓS-GRADUAÇÃO EM SANEAMENTO, MEIO AMBIENTE E RECURSOS HÍDRICOS

PROCESS INTENSIFICATION IN THE REFINERY EFFLUENT TREATMENT USING A PHOTOCATALYTIC MEMBRANE REACTOR

Caique Prado Machado de Oliveira

Belo Horizonte
2019

PROCESS INTENSIFICATION IN THE REFINERY EFFLUENT TREATMENT USING A PHOTOCATALYTIC MEMBRANE REACTOR

Caique Prado Machado de Oliveira

Caique Prado Machado de Oliveira

PROCESS INTENSIFICATION IN THE REFINERY EFFLUENT TREATMENT USING A PHOTOCATALYTIC MEMBRANE REACTOR

Dissertação apresentada ao Programa de Pós-graduação em Saneamento, Meio Ambiente e Recursos Hídricos da Universidade Federal de Minas Gerais, como requisito parcial à obtenção do título de Mestre em Saneamento, Meio Ambiente e Recursos Hídricos.

Área de concentração: Meio Ambiente

Linha de pesquisa: Caracterização, prevenção e controle da poluição

Orientadora: Drª. Míriam Cristina Santos Amaral
Co-orientador: Dr. Marcelo Machado Viana

Belo Horizonte
Escola de Engenharia da UFMG
2019

Caique Prado Machado de Oliveira

PROCESS INTENSIFICATION IN THE REFINERY EFFLUENT TREATMENT USING A PHOTOCATALYTIC MEMBRANE REACTOR

Dissertation presented to the Post-graduate Program in Sanitation, Environment and Water Resources of the Federal University of Minas Gerais, as a partial requirement to obtain the Master's degree in Sanitation, Environment and Water Resources.

Focus area: Environment

Research line: Characterization, prevention and control of pollution

Advisor: Profª. Drª. Míriam Cristina Santos Amaral
Co-advisor: Prof. Dr. Marcelo Machado Viana

Belo Horizonte
School of Engineering, Federal University of Minas Gerais
2019

Oliveira, Caique Prado Machado de.
O48p Process intensification in the refinery effluent treatment using a photocatalytic membrane reactor [recurso eletrônico] / Caique Prado Machado de. - 2018.
1 recurso online (xi, 80 f. : il., color.) : pdf.

Orientadora: Míriam Cristina Santos Amaral.
Coorientador: Marcelo Machado Viana.

Dissertação (mestrado) - Universidade Federal de Minas Gerais, Escola de Engenharia.

Bibliografia: f. 64-80.

Exigências do sistema: Adobe Acrobat Reader.

1. Engenharia sanitária - Teses. 2. Meio ambiente - Teses. 3. Dióxido de titânio - Teses. I. Amaral, Míriam Cristina Santos. II. Viana, Marcelo Machado. III. Universidade Federal de Minas Gerais. Escola de Engenharia. IV. Título.

CDU: 628(043)

Ficha catalográfica: Biblioteca Profº Mário Werneck, Escola de Engenharia da UFMG

UNIVERSIDADE FEDERAL DE MINAS GERAIS
Escola de Engenharia
Programa de Pós-Graduação em Saneamento, Meio Ambiente e Recursos Hídricos
Avenida Antônio Carlos, 6627 - 4º andar - 31270-901 - Belo Horizonte – BRASIL
Telefax: 55 (31) 3409-1882 - posgrad@desa.ufmg.br
http://www.smarh.eng.ufmg.br

FOLHA DE APROVAÇÃO

Process Intensification In The Refinery Effluent Treatment Using a Photocatalytic Membrane Reactor

CAIQUE PRADO MACHADO DE OLIVEIRA

Dissertação defendida e aprovada pela banca examinadora constituída pelos Senhores:

Profa MIRIAM CRISTINA SANTOS AMARAL MORAVIA

Prof. MARCELO MACHADO VIANA (COORIENTADOR)

Profa LUCILAINE VALÉRIA DE SOUZA SANTOS

Prof. GUILHERME OLIVEIRA SIQUEIRA

ANA CLÁUDIA FIGUEIRAS PEDREIRA DE CERQUEIRA

Aprovada pelo Colegiado do PG SMARH

Prof. Antonio Teixeira de Matos
Coordenador

Versão Final aprovada por

Profª. Miriam Cristina Santos Amaral Moravia
Orientadora

Belo Horizonte, 30 de julho de 2019.

AGRADECIMENTOS

Dizer que sou profundamente honrado e que agradeço a Deus é pouco. Dele veio e vem meu sustento e força diários e a fonte de inspiração a cada manhã para que mais esta fase fosse concluída. É Dele que provém meus dons, a luz que me ilumina e dá clarividência. O autor do dom da vida e A razão de todas as coisas. À Ele, minha gratidão sem fim.

À minha orientadora Míriam, minha gratidão mais sincera! Obrigado por todas as oportunidades concedidas, pela confiança em mim depositada, generosidade gratuita e disponibilidade constante e irrestrita ao passar seus conhecimentos e por ser exemplo de profissional em quem me espelho.

Ao meu co-orientador, Marcelo, registro meu honesto apreço e agradecimento. Obrigado por abraçar mais essa etapa da minha vida junto de mim e ser sempre essa fonte de conhecimento e generosidade. Obrigado por ter me concedido a primeira oportunidade científica e ter aberto as portas do mundo acadêmico que tanto me fascinou.

Agradeço de maneira incomensurável a meus pais: Geraldo e Fiora. Sem eles, certamente eu não conseguiria concretizar ou consolidar meus projetos. Obrigado por serem esses mestres da vida que me ensinaram e ensinam as maiores lições. Vocês são meu suporte, sustento e maiores incentivadores. Obrigado por TUDO que fizeram e fazem por mim. Todo meu empenho e tudo que faço é para vocês. Tenho o maior orgulho desse mundo de ser filho de vocês. Meu profundo amor, meu mais sincero carinho!

Ao meu irmão Victor pela amizade e parceria sempre presentes. Conversas instrutivas, orientações e pelos projetos juntos!

Aos professores do Desa que contribuíram para minha formação e aprimoramento do trabalho. Em especial ao professor Eduardo por gentilmente fornecer suas membranas recicladas.

Aos professores da banca: Dra. Ana Cláudia Cerqueira, Dra. Lucilaine Santos e Dr. Guilherme Siqueira por gentilmente aceitarem o convite de avaliar e contribuir com o melhoramento deste trabalho.

Aos amigos do laboratório GEAPS, pelo auxílio nas mais diversas demandas, por me acolherem tão bem e constituírem um grupo tão cooperativo. Agradeço de maneira especial à Letícia e ao

Gabriel que foram fonte de apoio em demasia relevantes nesse trabalho e tornaram os dias muito mais leves. Mais do que colegas no projeto, vocês hoje são amigos a quem destino meu carinho e torcida. Agradeço também à Priscila pelo auxílio sempre carinhoso e cooperação no projeto.

Aos amigos do Laboratório 219 do DQ pelas contribuições na síntese e caracterização do catalisador e pelos momentos de convívio prazerosos.

À todos meus familiares e amigos. Em particular, Mayra e Yasmim por serem irmãs da vida que carrego em parceria nos últimos anos que compartilham da minha mesma rotina acadêmica. Por me acompanharem em cada passo dessa etapa, nas conversas afetuosas, nos desideratos projetos de futuro e apoio constante.

À PUC Minas pela parceria na realização das análises de FTIR.

Ao Centro de Microscopia da UFMG pelas análises lá executadas.

Ao Conselho Nacional de Desenvolvimento e Pesquisa (CNPq) pela bolsa concedida.

Enfim, agradeço a todos que contribuíram direta ou indiretamente para esse trabalho!

Fica aqui o meu mais honesto obrigado!

RESUMO

A primeira parte do presente trabalho apresenta uma síntese ambientalmente amigável de nanopartículas de TiO_2 assistida por microondas, a partir de tetracloreto de titânio e água, com potencial para tratamento de efluentes de refinaria de petróleo. Partículas nanocristalinas de anatásio com tamanho médio de cristalito de 14 nm foram obtidas de acordo com a caracterização por DRX, MET e EELS. A atividade fotocatalítica do catalisador foi testada primeiramente pela degradação da molécula padrão de azul de metileno e 95% de degradação foram verificados após 300 minutos de reação. Testes cinéticos com o corante indicaram ajuste à cinética de primeira ordem. O permeado de UF de um Biorreator de Membrana tratando efluente real de refinaria de petróleo constituído majoritamente de compostos biologicamente recalcitrantes foi submetido a fotodegradação na presença do catalisador sintetizado sob irradiação UV-C. As maiores porcentagens de remoção de COT e NT obtidas foram de 32% e 67%, respectivamente, em condições de pH igual a 10 e concentração de catalisador de 100 mg L^{-1} em 90 minutos de reação. Para essa condição, a *Electric Energy per Order* (EE_0) calculada foi 356,29 KWh m^{-3} $ordem^{-1}$. O catalisador exibiu estabilidade na fotoatividade durante 4 ciclos. Na segunda parte do estudo, um sistema híbrido denominado Reator Fotocatalítico de Membrana (PMR) foi construído e testado para tratamento do efluente previamente mencionado. A configuração do PMR baseou-se na utilização do catalisador dióxido de titânio sintetizado por via mais limpa e membranas de osmose inversa recicladas por oxidação química com hipoclorito de sódio. O sistema se mostrou eficiente na remoção de compostos recalcitrantes do permeado de UF com valores de até aproximadamente 60% de remoção de DQO. Verificou-se que a fotocatálise exerce o maior impacto na remoção de matéria orgânica (21%) quando comparada aos valores de fotólise com luz UV (15%) e somente separação pela membrana (9%). Os fluxos de permeado da membrana reciclada permaneceram praticamente constantes nos testes com a presença do catalisador no PMR, mostrando que este reduz a incrustação, confirmada também pela resistência do fouling 7,3 vezes menor nos testes executados com a presença do óxido. Não foram detectados indícios de que o catalisador danificou a estrutura da membrana. Ao contrário, foram verificadas estabilidades nos fluxos e na fotocatálise pelos testes de reuso. As análises de MEV da membrana antes da permeação revelaram uma estrutura não rugosa. Alterações morfológicas não foram observadas na superfície da membrana após permeações. No entanto, depósitos de TiO_2 foram visualizados e confirmados por EDS. A análise de EDS em vários campos do permeado do PMR não identificou o elemento titânio mostrando que a membrana reciclada é capaz de reter o catalisador. Os compostos presentes no efluente estão principalmente associados a produtos microbianos como SMPs e EPS que tiveram suas concentrações reduzidas com base no desaparecimento das bandas 3300 cm^{-1}, 1620 cm^{-1} e 609 cm^{-1} do espectro de infravermelho. Os dados obtidos mostraram que o sistema é uma tecnologia promissora para a remoção de matéria orgânica recalcitrante residual do permeado do UF-MBR e tem potencial uso como etapa prévia aos processos de polimento do efluente de refinaria com vistas ao reuso.

Palavras-chave: dióxido de titânio; efluente de refinaria; síntese microondas, membrana reciclada; reator fotocatalítico de membrana, compostos recalcitrantes.

ABSTRACT

The first part of the present paper presents an environmentally friendly synthesis of TiO_2 nanoparticles assisted by microwave from titanium tetrachloride and water with potential for oil refinery wastewater treatment. Anatase nanocrystalline particles with a mean crystallite size of 14 nm were obtained according to XRD, TEM and EELS characterization. The photocatalytic activity of the catalyst was tested first by degradation of the standard methylene blue molecule and 95% degradation was verified after 300 minutes of reaction. Kinetic tests with the dye indicated adjustment to first order kinetics. The UF permeate of a Membrane Bioreactor treating real refinery wastewater composed largely of biologically recalcitrant compounds was subjected to photodegradation in the presence of the catalyst synthesized under UV-C irradiation. The highest percentages of TOC and TN removal were 32% and 67%, respectively, under pH conditions equal to 10 and catalyst concentration of 100 mg L^{-1} in 90 minutes of reaction. For this condition, the Electric Energy per Order (EE_0) calculated was 356.29 KWh m^{-3} $order^{-1}$. The catalyst exhibited stability in photoactivity for 4 cycles. In the second part of the study, a hybrid system called Photocatalytic Membrane Reactor (PMR) was constructed and tested for treatment of the previously mentioned effluent. The PMR configuration was based on the use of the cleaner synthesized titanium dioxide catalyst and reverse osmosis membranes recycled by chemical oxidation with sodium hypochlorite. The system proved to be efficient in the removal of UF permeate recalcitrant compounds with values up to 60% of COD removal. It was verified that photocatalysis exerts the greatest impact on the removal of organic matter (21%) when compared to photolysis with UV light (15%) and membrane separation only (9%). The permeate fluxes of the recycled membrane remained practically constant in the tests with the presence of the catalyst in the PMR, showing that it reduces the fouling, also confirmed by the fouling resistance 7.3 times lower in the tests performed with the presence of the oxide. No evidence was detected that the catalyst damaged the membrane structure. In contrast, stabilities in fluxes and photocatalysis were verified by reuse tests. SEM analyzes of the membrane prior to permeation revealed a non-rough structure. Morphological changes were not observed on the membrane surface after permeations. However, TiO_2 deposits were visualized and confirmed by EDS. Analysis of EDS in various fields of the PMR permeate did not identify the titanium element showing that the recycled membrane is able of retaining the catalyst. The compounds present in the effluent are mainly associated with microbial products such as SMPs and EPS that had their concentrations reduced based on the disappearance of the bands 3300 cm^{-1}, 1620 cm^{-1} and 609 cm^{-1} of the infrared spectrum. The obtained data showed that the system is a promising technology for the removal of residual recalcitrant organic matter of the UF-MBR permeate before the polishing process of the petroleum refinery wastewater with a view to reuse.

Keywords: titanium dioxide; refinery effluent; microwave synthesis, recycled membrane; photocatalytic membrane reactor, recalcitrant compounds.

SUMÁRIO

LIST OF FIGURES

LIST OF TABLES

LIST OF ABBREVIATIONS, ACRONYMS AND SYMBOLS

ABS – Absorbance

ABS^{254} – Absorbance at 254 nm

AOP – Advanced Oxidative Process

API – American Petroleum Institute

COD – Chemical Oxygen Demand

COT – Carbono Orgânico Total

DQO – Demanda Química de Oxigênio

DRX – Difração de Raios X

EDR – Electro Dyalisis Reversal

EE_0 – Eletric Energy per Order

EPS – Extracellular Polymeric Substances

FTIR – Fourier Transformed Infrared

HRTEM – High Resolution Transmission Eletronic Microscopy

MBR – Membrane Bioreactor

MET – Microscopia Eletrônica de Transmissão

MEV – Microscopia Eletrônica de Varredura

MF – Microfiltration

MSP – Membrane Separation Processes

NF – Nanofiltration

NT – Nitrogênio Total

PMR – Photocatalytic Membrane Reactor

RO – Reverse Osmosis

SEM – Scanning Electron Microscopy

SMP – Soluble Microbial Products

TEM – Transmission Eletronic Microscopy

TGA – Thermogravimetric Analysis

TiO_2 – Titanium dioxide

TN – Total Nitrogen

TOC – Total Organic Carbon

UF - Ultrafiltration

UF-MBR – Ultrafiltration Membrane Bioreactor

UV – Ultraviolet

XRD – X-Ray Diffraction

CHAPTER 1

Introduction

1.1 Background

The propulsive mechanisms of the modern world are based on the pillars of innovation, technological breakthroughs, and development in a globalized context. At this juncture, there is also a scenario of each time less availability of raw materials, higher energy prices and more restrictive legislation for safer and environmentally less damaging practices. Reconciling such bases in sustainable growth is one of the major challenges facing the industry (KIM *et al.*, 2017; KEIL, 2018).

One of the widespread approaches to meet development goals in the current landscape is Process Intensification (PI). The term began to be used in the 80's by the group of Prof. Ramshal being defined as: "the design of an extremely compact plant that reduces both the main core item and the facility costs" (VAN GERVEN and STANKIEWICZ, 2009; WANG *et al.*, 2017) and has broadened its range of scope and today covers the changes that contribute to the increase of the efficiency and productivity in an equipment with a given volume or the reduction of the energy consumption in a given operation, as well as the minimization in the generation of by-products, effluents or tailings (COWARD *et al.*, 2018).

The integration of separation processes to chemical reactors is an excellent example of process intensification because a number of benefits are achieved in these configurations to the detriment of separated processes (DRIOLI, 2011; MENG *et al*, 2017). Membrane photocatalytic reactors (PMR), in particular, are a class of such integrated processes that combine photocatalytic oxidation with membrane filtration (MOZIA, 2010; LEONG *et al.*, 2014; MOLINARI *et al.*, 2017). Several advantages are obtained in the PMRs as higher reaction yields by shifting the chemical equilibrium by constant product separation of the reactants, more compact designs, extending the life of the catalysts, controlling the addition of one or two reactants in the reactor, separating the catalyst in the reactor after the reaction and its recovery, immobilization of the catalyst in the membrane and mitigation of the fouling in the membranes by the degradation of pollutants by the catalyst (DRIOLI, 2011; MENG *et al*, 2017).

One of the most widely used catalysts in the literature in heterogeneous photocatalysis at PMRs is titanium dioxide (TiO_2) because it presents high chemical stability, commercial availability and low cost (ANI *et al.*, 2018). The mechanism of action in the degradation of the pollutants by this catalyst occurs through the formation of hydroxyl radicals, thus consisting of an advanced oxidative process (ONG, *et al*, 2018).

When TiO_2 is irradiated by UV light, the electrons are excited from the valence band to the conduction band leaving positive gaps (also called holes) in the valence band (Fig. 1). Electrons and gaps migrate to the surface of the oxide and participate in a series of oxide-reduction reactions. Electrons reduce Ti (IV) to Ti (III) and, consequently, reduce oxygen adsorbed on the surface of TiO_2 generating superoxide radicals (O_2^-). Positive gaps react with water molecules generating hydroxyl radicals. Organic compounds may react with the formed radicals being oxidized to CO_2 and water, as described in equations (Eq. 1-5). Radicals also have the ability to inactivate microorganisms, bacteria and viruses (AHMED and RAIDER, 2018).

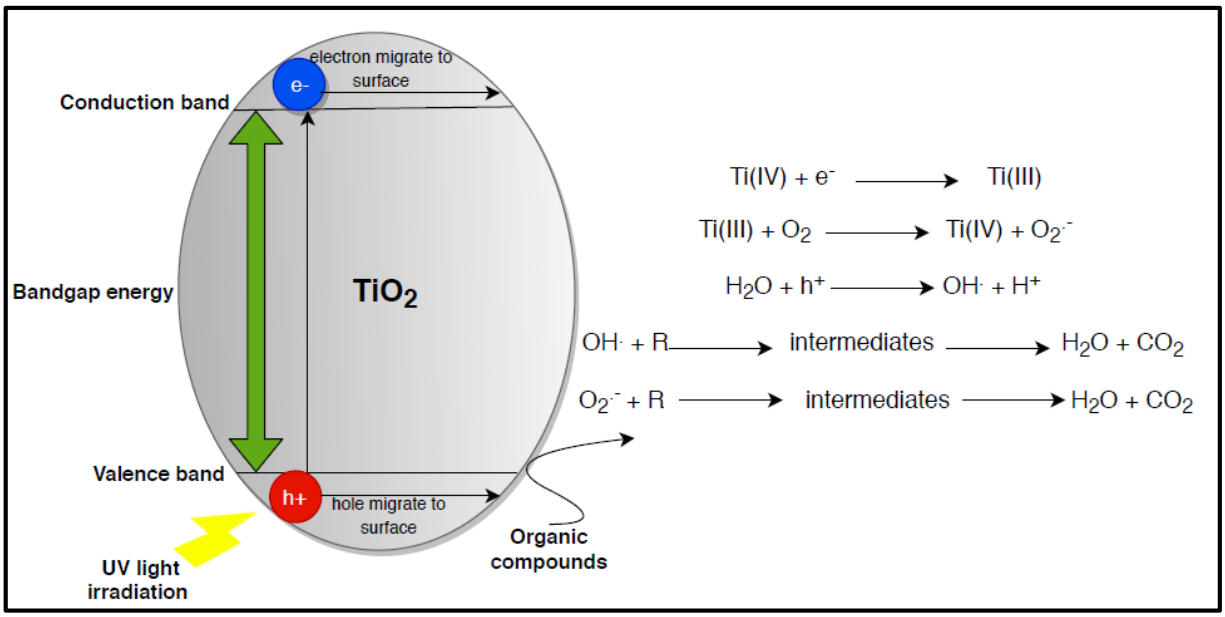

Figure 1: Schematic diagram of the pollutant degradation in the presence of the TiO_2 catalyst.

Source: Adapted from LEONG, *et al.* (2014).

$Ti(IV) + e^- \rightarrow Ti(III)$ Eq. (1)

$Ti(III) + O_2 \rightarrow Ti(IV) + O_2^{\cdot -}$ Eq. (2)

$H_2O + h^+ \rightarrow OH^{\cdot} + H^+$ Eq. (3)

$OH^{\cdot} + R \rightarrow intermediates \rightarrow H_2O + CO_2$ Eq. (4)

$O_2^{\cdot -} + R \rightarrow intermediates \rightarrow H_2O + CO_2$ Eq. (5)

The use of such a catalyst at the nanoscale is desirable because in these dimensions the surface/volume ratio is higher favoring photocatalysis. However, the functionality of the oxide with such a reduced size is limited because of its difficult maintenance in the system and

reusability (VIANA *et al.*, 2010). Thus, the conjugation of the processes that make use of it with membranes is an alternative with pronounced benefits, as previously mentioned.

Among the applications of the PMR's that use TiO_2, the treatment of oil refinery wastewaters is highlighted because this effluent presents in its composition a high concentration of aromatic and aliphatic hydrocarbons and associated to the presence of phenolic and recalcitrant compounds makes it difficult to be treated by biological processes (VENDRAMEL *et al.*, 2015). Refinery wastewater is considered the largest source of aquatic environmental pollution (WAKE, 2005), which shows the need for implementation of advanced treatment technologies that meet environmental launch standards and even generate reuse water (FARAJNEZHAD and GHARBANI, 2012).

Refinery effluents vary in composition depending on the type of raw oil and the refining process configuration (ALJUBOURY *et al.*, 2017). The traditional treatment occurs through physical operations and biological processes that are followed by polishing processes such as adsorption, membrane filtration and reverse osmosis. However, some recalcitrant compounds maintain even after more sophisticated processes as membranes bioreactors (AKPAN and HAMEED, 2013; NASSEH *et al.*, 2018). Thus, PMR indicates promising results in the degradation of persistent compounds from this effluent.

Most of the studies involving PMRs report the use of ultrafiltration (UF), microfiltration (MF) and nanofiltration (NF) polymer or ceramic membranes (HAIROM *et al.*, 2015; MOLINARI, LAVORATO and ARGURIO, 2017). But nothing was found regarding the use of recycled membranes in these systems. Some technologies, such as desalination by reverse osmosis (RO), for example, make use of an expressive number of membranes that are discarded after their lifespan (SHENVI, ISLOOR, ISMAIL, 2015). In 2016, the number of facilities with this technology was over 13,000 units worldwide (PAULA, 2017). Recycling such membranes for less noble purposes shows an environmentally friendly approach and their use as substituents to UF or MF, at low cost, in PMRs represents a major benefit for wastewater treatment operations in the industry (LAWLER, 2013; GARCÍA PACHECO, 2015).

Thus, given the above context, the development of a photocatalytic membrane reactor from nanoparticulate titanium dioxide produced by cleaner route, and reverse osmosis recycled membranes is a promising alternative for the treatment of refinery wastewater, especially for the removal of recalcitrant compounds, with a view to reuse in the plant itself.

1.2 Justification

The present work aims to propose a process for refinery wastewater tertiary treatment, based on the pillars of Process Intensification, combining membranes and photocatalyst in a Photocatalytic Membrane Reactor (PMR). The work aims to elucidate not only the applicability of the process for industrial reuse but also to evaluate the effectiveness of the synergistic effects of the catalyst on the membrane and the membrane on the catalyst.

The motivation found is based on the increase of water demand, associated with a decrease in the water supply and higher costs for the collection of raw water, as well as the presence of increasingly restrictive laws. In this context, industries prefigure as being prominent exponents of this demand. In particular, large oil refineries consume amounts in the order of 1 m^3 of fresh water per 1 m^3 of barrel processed (PETROBRÁS, 2018) to carry out the stages of treatment of the oil in obtaining the various products that come from it. It justifies the need to implement wastewater treatment in this segment that will allow reuse. Reuse that in addition to reducing the costs of the process as a whole, prints a substantial increase in the sustainability of the process, as well as mitigates some of its environmental impacts.

The refinery effluent, as it contains concentrations of pollutants sometimes toxic to microorganisms and recalcitrant compounds may be difficult to be treated by conventional processes. The potential of the use of advanced oxidative processes in this area is due to their possibility to promote the degradation of several molecules, leading to the mineralization of these molecules to carbon dioxide and water.

Titanium dioxide was chosen as the catalyst of the process because of its chemical stability and good performance under UV irradiation. Its synthesis in the nanoparticulate form is justified by the larger surface areas of the material in these dimensions which is a factor of relevance in the photocatalysis. The present study aims to identify and propose a solution to problems related to the use of such material at the nanoscale, through the membranes association.

The configuration of the Membrane Photocatalytic Reactor provides mutual benefits between the technologies. The membrane is a physical barrier to the catalyst and acts controlling the residence time of the compounds in the reaction. It also retains molecules that are not degraded. And in return, the catalyst promoting the decomposition of feed compounds reduces membranes fouling, which is a major operational problem. Such configuration for the treatment of refinery

wastewater tertiary treatment was not found in the literature by the use of a cleaner route for catalyst synthesis.

Another originality of the work refers to the use of recycled Reverse Osmosis (RO) membranes through sodium hypochlorite chemical oxidation in a PMR. Thus, a more sustainable destination is given to membranes that no longer play their role in reverse osmosis process with the possibility of their use as ultrafiltration or microfiltration membranes, therefore reducing their disposal.

The present study may contribute to the evaluation of the efficiency of Photocatalytic Membrane Reactors, comprising of suspended nanoparticulate TiO_2 and recycled reverse Osmosis membranes in the treatment of the refinery effluent.

1.3 Objectives

1.3.1 General objective

The aim of this work was to investigate the effectiveness of a Photocatalytic Membrane Reactor constituted by titanium dioxide nanoparticles and recycled reverse osmosis membranes for industrial wastewater tertiary treatment.

1.3.2 Specific objective

- To synthesize the nanoparticulate titanium dioxide (TiO_2) catalyst in the anatase crystallographic phase by a rapid microwave-assisted green route;
- To verify the photoactivity of the synthesized catalyst in the degradation of organic compounds;
- To construct a Photocatalytic Membrane Reactor (PMR) using the synthesized catalyst and the recycled reverse osmosis (RO) membrane;
- To verify the recycled RO membrane retention capacity to the synthesized photocatalyst;
- To evaluate the recycled RO membrane resistance to the oxidative conditions of the medium;
- To evaluate the performance of the constructed PMR regarding the removal of pollutants and the membrane permeate flow stability in the treatment of refinery wastewater after a Membrane Bioreactor (MBR) with a view to reuse;

- To carry out Eco toxicological tests to analyze the byproducts generated in photocatalysis;
- To measure the individual contributions of photolysis, adsorption, catalysis and membrane separation process in the PMR performance at Chemical Oxygen Demand (COD) removal.

1.4 Document Structure

The present study is structured in four chapters. Chapter 1 is introductory and provides a general contextualization of the theme as well as the justification and relevance of the work and its objectives. Chapter 2 presents the synthesis of the titanium dioxide catalyst through a cleaner route with an economy of reagents making the use of microwaves and evaluates the potential of this material for the degradation of organic compounds from refinery secondary wastewater, through the photocatalysis. Also in this chapter, the best conditions for the process are investigated and the energy consumption of the treatment is estimated. Chapter 3, in its turn, presents the construction of the Photocatalytic Membrane Reactor from the synthesized catalyst and recycled reverse osmosis membranes. The membrane retention capacity to the catalyst and the effects that the systems exert on each other (confinement of the nanoparticulate catalyst in the reaction medium by the membrane and decrease in the membrane fouling by means of the pollutants degradation by the catalyst) are evaluated. The efficiency of PMR treatment in the removal of recalcitrant compounds of UF permeate from a Membrane Bioreactor treating refinery wastewater is verified in this chapter. Finally, Chapter 4 presents the main conclusions drawn from the study and Chapter 5 the future perspectives from the work. Chapters 2 and 3 have been prepared in the format of articles, so that each one can be read independently.

CHAPTER 2

Coupling photocatalytic degradation using a green TiO_2 catalyst to Membrane Bioreactor for petroleum refinery wastewater reclamation

2.1 Introduction

Pollution control has been a major concern of the industrial sector given the high potential impact of its activities on the environment. The presence of more restrictive environmental laws, industry pressure for sustainable eco-friendly practices, increased catchment and treatment of water for productive processes, costs of effluent disposal, and water scarcity in some cases, has driven effluents reuse (SOUSA *et al.*, 2011; HODGES *et al.*, 2018; SZYMAŃSKI *et al.*, 2018).

The oil industry, in particular, has a high water consumption in its most diverse operations such as cracking and distillation, for example, thus generating a high volume of effluents. The reuse in this segment is, therefore, an alternative that can bring economic and environmental benefits (ALKMIM *et al.*, 2017; HANSEN *et al.*, 2018).

The traditional treatment occurs through mechanical methods and the biological processes are commonly used as a secondary treatment step being followed by polishing processes such as adsorption, membrane filtration and reverse osmosis (AKPAN and HAMEED, 2013; NASSEH *et al.*, 2018). However, due to the presence of a high concentration of aromatic and aliphatic hydrocarbons besides the presence of phenolic and recalcitrant compounds, the biological processes alone are not always able to meet the reuse quality (VENDRAMEL *et al.*, 2015).

The literature reports many works with technologies aiming the refinery wastewater treatment in order to reuse and Membrane Bioreactors (MBRs) are highlighted (ALKMIM *et al.*, 2015; ALSALHY *et al.*, 2015; ABASS *et al.*, 2018). MBRs consists in the combination of biological and membranes separations processes and are an ideal technology for non-potable reuse because of the superior quality effluent they produced compared to conventional clarification processes, due advantages like high sludge age and total removal of suspended solids (AMARAL *et al.*, 2014). Nevertheless, the rejection of low molecular weight compounds, ions and viruses by the ultrafiltration membranes (UF) in the MBRs are limited (HOLLOWAY *et al.*, 2014).

The MBR permeate may contain recalcitrant organic compounds, ions and biological organic waste as soluble microbial products (SMP) and extracellular polymeric substances (EPS) that may affect subsequent polishing steps by other membrane separation processes such as reverse osmosis (RO), nanofiltration (NF) and reverse electrodialysis (EDR) for reuse in cooling towers or boilers, for example (COSENZA *et al.*, 2013; SOUZA *et al.*, 2016). These compounds are

potential fouling agents that reduce permeate flux and raise transmembrane pressure, thereby increasing cleaning frequencies and membrane changes, increasing operating costs and energy consumption. In addition, such compounds when rejected by RO, NF and EDR membranes make it difficult to treat the concentrate because the presence of organic matter has inhibitory effects on crystallization, which consists on the process of treating concentrates of membrane separation processes (MOSER *et al.*, 2018).

Based on this, the removal of residual organic matter of the UF effluent produced by the Membrane Bioreactor prior to the polishing processes is necessary and the advanced oxidative processes (AOPs) are shown to be promising for the pretreatment of membrane separation processes such as OI, NF and EDR (KHAN *et al.*, 2015; ESTRADA-ARRIAGA *et al.*, 2016). The AOPs have attracted special attention in the water and wastewater treatment for being efficient in the degradation of toxic and recalcitrant pollutants and by the possibility to convert them to simple and non-dangerous inorganic molecules and even may eliminate some heavy metals by precipitation in metal hydroxides (ANI *et al.*, 2018). The mechanism of the process occurs by the formation of hydroxyl radicals that are the strongest oxidizing agents in aqueous solution after fluorine (ONG *et al.*, 2018).

Among the different configurations of AOPs processes, the heterogeneous photocatalysis with titanium dioxide (TiO_2) is highlighted because the oxide is one of the most versatile materials that adds the advantages of low cost, non-toxicity, photostability and ease of synthesis and use. Thus, its applications extend from the degradation of organic pollutants to energy generation (ALJUBOURY *et al.*, 2016).

The oxide is found in nature in three polymorphs: anatase, rutile and brookite. The anatase phase is the most extensively studied due to its high photoactivity, low electron-hole recombination rate and nanometric stability (CHEN *et al.*, 2009). The preference for use of the material at the nanoscale is for the reason that nanoparticles have a high surface/volume ratio and high surface areas implying higher reaction rates (VIANA *et al.*, 2010; KAPILASHRAMIM *et al.*, 2014).

When TiO_2 is irradiated by UV light, its electrons (e^-) are excited from the valence band to the conduction band leaving positive gaps (h^+) (also called holes) in the valence band (VB). Electrons and gaps migrate to the surface of the oxide and participate in a series of oxi-reduction reactions. Electrons reduce Ti^{4+} (IV) to Ti^{3+} (III) and, consequently, reduce oxygen adsorbed

on the surface of TiO_2 generating superoxide radicals (O_2^-). Positive gaps react with water molecules generating hydroxyl radicals (OH^-). Organic compounds may react with the formed radicals being oxidized to CO_2 and water. Radicals also have the ability to inactivate microorganisms, bacteria and viruses (AHMED and HAIDER, 2018; YE *et al.*, 2018).

The TiO_2 performance can be influenced by several parameters such as the surface area of the material, crystalline structure and density of surface hydroxyl groups, all of which may differ according to the route of synthesis adopted (BESSEKHOUAD *et al.*, 2003, BEHNAJADY *et al.*, 2009; NOMAN *et al.*, 2018).

Different methods of TiO_2 synthesis have been studied, such as the sol-gel process, hydrothermal method, solvothermal, reverse microemulsions and microwave (ZHANG *et al.*, 2009; KOMARNENI *et al.*, 2010; ZUBIETA *et al.*, 2011; ELSELLAMI *et al.*, 2017). Methods as hydrothermal or sol-gel, for example, require long synthesis times and high calcination temperatures, as well as the use of multiple steps and reagents, which can generate aggregation of the particles and contamination of the product (LI *et al.*, 2010; CABELLO *et al.*, 2017).

An alternative and faster route of synthesis, with lower energy consumption and more efficient is the one that makes use of microwaves (WANG *et al.*, 2012; SHEN *et al.*, 2014). Microwave reactions were reported as reducing the time in hydrothermal synthesis by 1/3, besides producing unique crystals and lower losses (CORRADI *et al.*, 2005; MANFROI *et al.*, 2014). In this method, the microwave energy is transmitted directly to the material, through interactions with the magnetic field generating homogeneous nucleation and uniform growth of the nanoparticles (BHATTACHARYA and BASAK, 2016; MIRZAEI and NERI, 2016).

Among the various applications of TiO_2, its use in the treatment of petroleum refinery effluent deserves to be highlighted (KHAN *et al.*, 2015, ANI *et al.*, 2018). This is because the photocatalysis using TiO_2 indicates promising results in the degradation of persistent compounds from this effluent. Mohd Hir *et al.* (2011) obtained 73% degradation of benzene, toluene and xylene in the treatment of refinery effluent using TiO_2. Topare *et al.* (2015) achieved a 60% Chemical Oxygen Demand (COD) removal from the refinery effluent by TiO_2/UV treatment.

The literature reports many studies involving the degradation of isolated molecules by TiO_2 catalyst, in most cases, the commercial one. But there is a lack of thematic in the case of real complex matrix effluents and catalysts developed through cleaner routes. Moreover, the major

part of the studies involving AOPs in the refinery effluent treatment uses reagents that are consumed in the reaction, differently of what happens in the heterogeneous catalysis with titanium dioxide.

Considering the panorama of the scientific researches, the present work presents the synthesis of TiO_2 nanoparticles in an environmentally friendly way through a fast route and with reduced consumption of reagents assisted by microwave. Anatase single-phase nanoparticles were obtained and assessed structurally and morphologically. The photocatalytic activity of the catalyst was evaluated by the degradation of methylene blue as a model pollutant molecule and the kinetic degradation constant determined for subsequent reactor design studies. Tests of catalyst application were carried out in the degradation of real refinery wastewater treated in a Membrane Bioreactor and the process efficiency was measured by Total Organic Carbon (TOC) and Total Nitrogen (TN) removals. In order to determine the best degradation conditions, a series of experiments were conducted varying the pHs of the medium and catalyst concentration. The results obtained in this study associated to the ease of production of the material, in a clean way and with the reduction of reagents can help in the application of nanoparticles in the removal of refinery effluent recalcitrant contaminants.

2.2 MATERIALS AND METHODS

2.2.1 Refinery wastewater post MBR

The refinery wastewater was collected in a Brazilian oil refinery after a primary treatment for oil removal by an American Petroleum Institute (API) separator and dissolved air flotation. After the primary treatment, the wastewater was treated at room temperature (25 ± 1 °C) by a bench-scale Membrane Bioreactor (MBR) which comprises a 3.36 L (effective volume) biological reactor with constant aeration around 0.5 $Nm^3\ h^{-1}$ in which a hollow fiber UF membrane (ZeeWeed 1 – GEPVDF, average pore diameter: 0.04 μm, area: 0.047 m^2) was submerged. The biological sludge concentration was maintained at approximately 3.7 $g\ L^{-1}$ and the pH adjusted to around 7.0. The MBR was operated under hydraulic retention time of 6 hours and sludge retention time of 45 days. The ultrafiltration permeate flow rate was maintained at 0.55 $L\ h^{-1}$.

The MBR permeates were the samples used for the photodegradation tests with TiO_2. To avoid changes in the features, they were stored in a refrigerator at 4 °C. Its main physicochemical characteristics are described in table 1.

Table 1– Main physicochemical characteristics of the UF permeate from MBR treating refinery wastewater

Parameter	Unit	Mean ± Standard Deviation
COD	$mgO_2\ L^{-1}$	45.4 ± 24.8
DOC	$mg\ L^{-1}$	15.4 ± 8.7
IC	$mg\ L^{-1}$	6.7 ± 2.2
Alkalinity	$mg\ L^{-1}\ CaCO_3$	31.4 ± 31.9
Chloride	$mg\ L^{-1}$	598.0 ± 167.9
Sulfate	$mg\ L^{-1}$	198.6 ± 31.1
Ammonia	$mg\ L^{-1}$	0.9 ± 0.7
Total Nitrogen TN	$mg\ L^{-1}$	36.2 ± 4.9
Conductivity	$\mu S\ cm^{-1}$	2393.1 ± 486.4
Color	$PtCo\ L^{-1}$	44.2 ± 16.8
Turbidity	NTU	0.77 ± 0.11

DOC: dissolved organic carbon; IC: inorganic carbon

2.2.2 Reagents

The reagents used in the subsequent steps were 1.10-Phenatroline (Fluka); Ammonium hydroxide (NH_4OH) (Sigma-Aldrich); Ferric Chloride Hexahydrate ($FeCl_3.6H_2O$) (Synth); Methylene blue (Exodo Científica); Potassium Oxalate ($K_2C_2O_4$) (Synth); Sodium acetate trihydrate ($CH_3COONa.3H_2O$) (Fluka); Sodium Hydroxide (NaOH) (Dinâmica); Titanium tetrachloride ($TiCl_4$) (Merck); Sulfuric acid (H_2SO_4) (Vetek). All solutions were prepared with Milli Q ultra pure water.

2.2.3 Photocatalyst synthesis

The catalyst was synthesised based on the study by Li and Zeng (2011) using a modified route with a reduced use of chemical reagents and microwave irradiation. First, 6 mL of titanium tetrachloride ($TiCl_4$, Merck) was added in 150 mL of distilled water in a round-bottom flask immersed in an ice bath. Subsequently, 10 mL of ammonium hydroxide (NH_4OH, Sigma-Aldrich) was added to the mixture to adjust the pH to 8. The system was allowed to stir in the

bath for 30 min. Subsequently, the reaction mixture was placed in a microwave oven (Milestone Start D) and subjected to a heating ramp to 80 °C for 6 min. This temperature was then maintained for 4 min. Subsequently, another cooling ramp was carried out to 50 °C for 20 min. The obtained material was washed with water and centrifuged at 3500 rpm several times until neutral pH was achieved. It was then kept in a kiln for drying at 85 °C for 2 h and calcined at 400 °C according to a programmed heating ramp of 25 °C to 400 °C in 1 hour and 15 minutes, kept in 400 °C for 2 hours and finally 400 °C to 25 °C in 1 hour. Calcination was used to remove byproducts from synthesis

2.2.4 Description of the experimental apparatus

The experimental apparatus for the tests consisted of the reactor, a diaphragm pump (Flojet D2235) and a rotameter to verify the circulation flow, as shown in Figure 2. The photodegradation reactions were performed in a cylindrical PurePro Ultraviolet water sterilizer reactor (50.5 × 320 mm and 280 mL capacity) with a quartz tube inside. A low-pressure mercury vapor lamp (6 W), emitting radiation at 254 nm, was connected to the quartz tube.

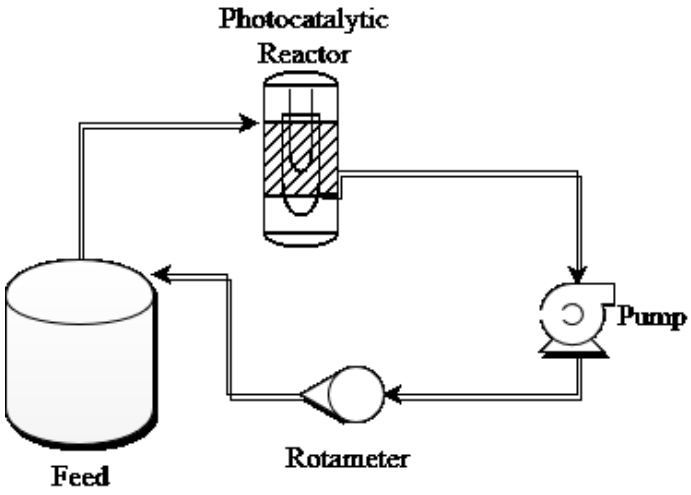

Figure 2: Schematic diagram of the apparatus of the degradation tests.

2.2.5 Photocatalyst performance

2.2.5.1 Methylene blue photodegradation

To verify the effectiveness of UV light in the photolysis promoted by the reactor, as well as evaluation of the performance of the catalyst, tests using the methylene blue dye as an organic model molecule were done. 200 mL of 20 mg L^{-1} solution of the dye were put into circulation in the reactor. Aliquots of the solution were collected every 30 minutes for reading at the

wavelength of 661 nm (lambda of maximum absorption of methylene blue) on the UV-Vis spectrophotometer (Perkin Elmer UV/Vis Lambda Spectrophotometer) until a 240 minutes test were completed. With a calibration curve the decay of the catalyst concentration was determined over time. The same test was carried out by adding 240 mg of the TiO_2 catalyst to the methylene blue solution, with the exception of leaving the reaction system for one hour in the dark to determine the adsorption of the dye to the catalyst.

2.2.5.2 UF permeate from MBR purifying

The tests using the wastewater were performed at 25 °C. To determine optimized conditions for reduction of the organic matter of the effluent, various pH values of the medium and different catalyst concentrations were tested. At a concentration of 100 mg L^{-1} of the catalyst, tests were carried out at pHs 2, 4, 6, 8 and 10. And at the pH 10, tests of 100 mg L^{-1}, 125 mg L^{-1} and 150 mg L^{-1} catalyst concentration were developed. The pHs were corrected with solutions of NaOH 0.1 mol L^{-1} and H_2SO_4 0.1 mol L^{-1}. After the batches, the treated effluent was analyzed in terms of TOC and TN. In all tests, the reaction time was 90 minutes and the treated effluent volume was equal to 150 mL. The stirring was maintained in the reaction system by the current formed by the use of the pump. The percentage of TOC removal was calculated according to Equation 6:

$$R\% = \frac{TOC_0 - TOC_f}{TOC_0} x\ 100 \qquad \text{Eq. (6)}$$

Where: $R\%$ is the percentage TOC removal

TOC_0 is the initial TOC

TOC_f is the final TOC

To determine the total nitrogen removal, the calculation procedure analogous to that described in equation 6 was performed.

The energy consumption is an important information to be analyzed in process, which uses electric energy as the heterogeneous catalysis. Therefore, the Electric Energy per Order (EE_o) is a very useful and informative figure of merit to measure the balance between the energy required to achieve a certain TOC removal. Originally, EE_0 is defined as the number of kilowatt hours of electrical energy required to reduce the concentration of a pollutant by 1 order of magnitude (90%) in a unit volume of contaminated water. Specifically at this work, as all the

experiments at different catalyst doses and pHs were conducted in 90 minutes, the EE_0 was calculated considering the TOC removal achieved at this time as described by Equation 7:

$$EE_0 = \frac{P \text{ x } t \text{ x } 1000}{V \text{ x } 60 \text{ x } log\frac{C_0}{C}} \quad \text{Eq. (7)}$$

Where P is the electric input power (KW) from UV lamp to the AOP system, t is the irradiation time (min), V is the volume of treated effluent (L) in reactor and C_o and C are initial and final TOC concentrations (mg L^{-1}), respectively.

The term that uses logarithm is due to the fact that EE_0 was concept and appropriated to be used in the first-order kinetic regime of AOPs, when the low pollutant concentrations are solved in solution (BEHNAJADY *et al.*, 2009).

2.2.6 Analytical methods

The catalyst was characterized by X-ray diffraction (Shimadzu XRD-7000 X-ray diffractometer, copper tube Kα (λ = 1.54056 Å), voltage of 30 kV, current of 30 mA and scanning speed 0.05 ° s^{-1}) to verify the crystallographic phase of the formed oxide and estimate the average crystallite size by the Debye-Scherrer equation. Sodium Chloride (NaCl) was used as a pattern in these tests (CHAUHAN, KUMAR and CHAUDHARY, 2012).

Transmission Electron Microscopy (FEI TECNAI G2-20 microscope with LaB_6 thermionic filament tube, acceleration voltage of 200 KV) was performed to verify the morphology and distribution of the particle sizes of the material. The samples were prepared by dispersing them in ethanol using sonication, and then one drop of the suspension was deposited on a carbon-coated copper grade.

The raw effluent as well as the flows treated in the photodegradation were characterized by pH using Qualxtron QX 1500 pHmeter; conductivity in the Hanna conductivity meter; TOC (5310B) and TN (D8083) in the Shimadzu TOC-V CNP TOC analyzer equipment, in accordance with the Standard Methods for the Examination of Water and Wastewater (APHA, 2012).

The luminous intensity of the mercury vapor lamp was determined by the actinometric test using the potassium ferrioxalate reagent, as described by Murov (1973). The light intensity determined was $5.5x10^{-5}$ Einstein min^{-1}.

Concentrations of the solutions in the actinometric test and degradation of the methylene blue dye were measure by UV-Vis PerkinElmer spectrophotometer, Lambda XL, by means of calibration curves.

2.2.7 Statistical analysis

A Spearman rank correlation test ($p < 0.05$) was used for correlation analysis between the parameters pH, catalyst dose and TOC and TN removals in the refinery effluent. The statistical analyses were performed by Statistica 10.0 Software.

2.3 RESULTS AND DISCUSSION

2.3.1 Catalyst characterization

Figure 3 shows the diffractogram of the synthesized TiO_2 photocatalyst. All the obtained peaks are well defined corresponding to the crystallographic planes (101), (103), (200), (105), (213), (116), (107) characteristics of anatase phase and are in agreement with the diffraction pattern PDF 1-562. This result evidences that the adopted route prioritizes the formation of the pure anatase phase, since no brookite or rutile peaks have been identified.

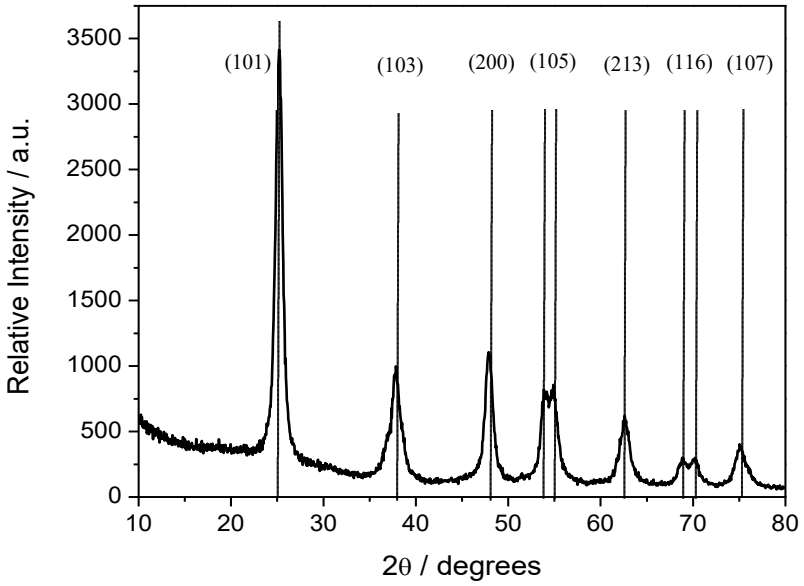

Figure 3: XRD patterns of synthesized TiO_2 nanoparticles.

The synthesis developed in the present work is aligned with the principles of cleaner methods, since pure crystalline titanium dioxide in the anatase phase was obtained with saving of reagents, starting only from titanium tetrachloride and water. In addition, the microwave

technique makes it possible to obtain the material in a shorter time when compared to conventional techniques. It was necessary hours while days are required in other techniques (ZHANG *et al.*, 2016). Mohadesi and Ranjbar (2015) also obtained materials with a single phase, however, their precursors were titanium tetraisopropoxide, water and nitric acid. In addition, other authors using a microwave-based synthesis technique obtained polymorphs from precursors such as titanium tetraisopropoxide (BREGADIOLLI, *et al.*, 2017) and tetra-n-butyl titanate (LI *et al.*, 2010). The average crystallite size estimated by the Debye-Scherrer equation was 14 nm based on the most intense peak relative to the anatase phase (101) located at 2θ = 25.10°.

TEM images (Fig. 4) have shown that the synthesized particles are of the nanometric order and are agglomerated. Such agglomeration may be related to the absence of steps such as sonication after synthesis (BREGADIOLLI *et al.*, 2017), as well as being a result of the high reaction rates in the microwave processes (CABELLO, DAVOGLIO and PEREIRA, 2017).

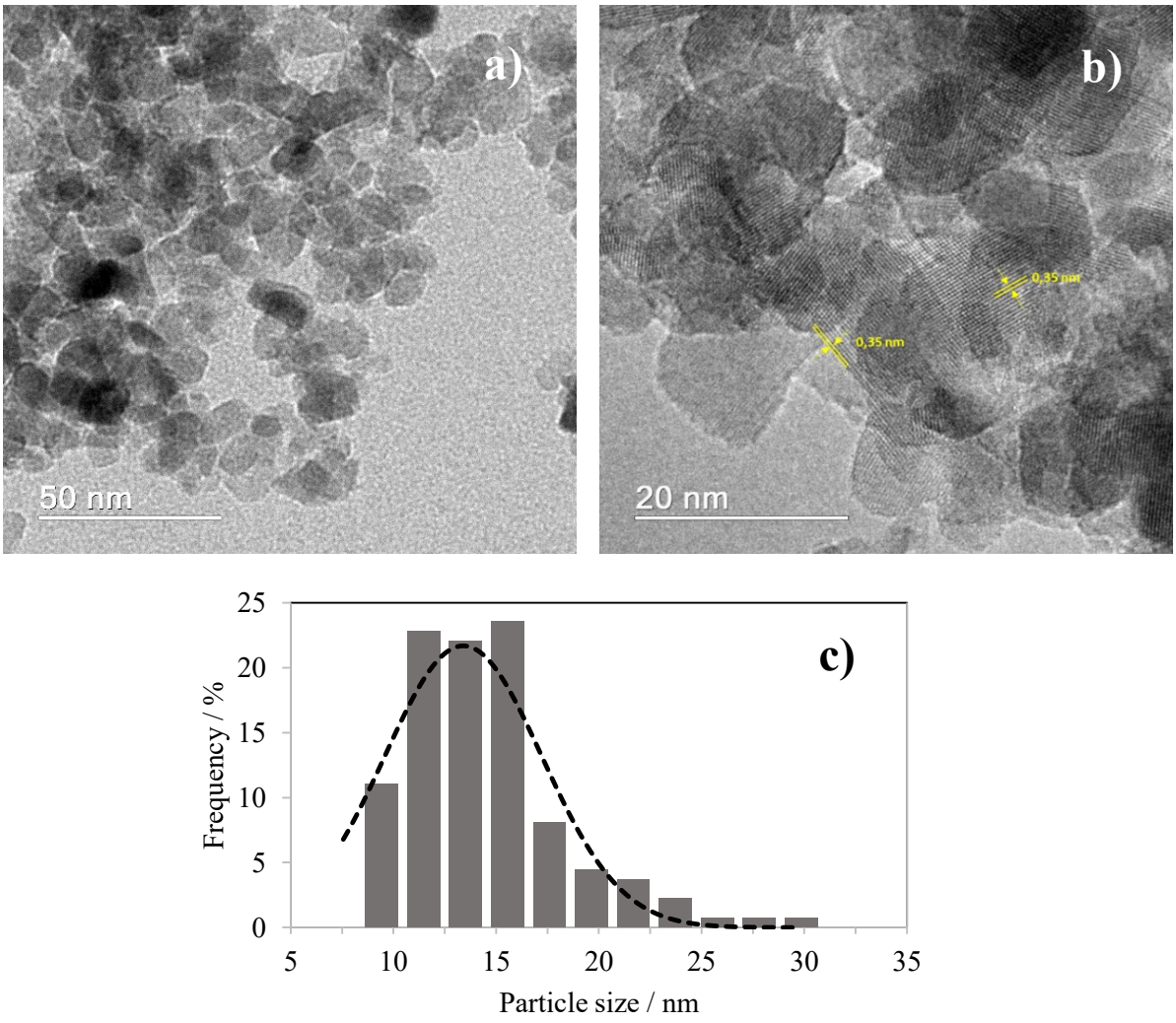

Figure 4: TEM images of synthesized TiO_2 (a-b), histogram of particle size distribution (c).

By the analysis of Figures 4-a) and 4-b) it is possible to note that the particles have dimensions between 8 and 30 nm, which was confirmed by the image study carried out with the aid of ImageJ software, whose product is the histogram shown in Figure 4-c) (140 particles analyzed). In the histogram it can be verified that the highest percentage of the particles has dimensions between 11 and 16 nm and through the normal distribution curve, it can be seen that the crest (average) occurs around 14 nm. This value is in agreement with that obtained by the Debye-Scherrer equation. Due to the fact that the material was calcined, the particles were expected to be above 10 nm (FALK, *et al.*, 2018). From the high-resolution image (Figure 4-b), the interplanar spacing in the well-defined crystals was measured and the distance found was 0.35 nm corresponding to the (101) plane of the anatase.

Figure 5-a) shows the electron diffraction pattern of the sample and confirms its polycrystallinity by the presence of concentric rings, indicating crystallographic planes that grew in different orientations. Each of the rings was indexed according to PDF 1-562 and the values correspond to the TiO_2 in the anatase phase. The intense brightness of the well-defined rings reveals that the material has completely crystallized. The electron loss spectrum (EELS) obtained from the sample (Fig. 5-b) coincides with the spectrum available in the Atlas EELS for TiO_2 (MATSUMOTO *et al.*, 2013; AKITA and KOHYAMA, 2014), corroborating the other results that the sample consists of titanium and oxygen in the form of titanium dioxide.

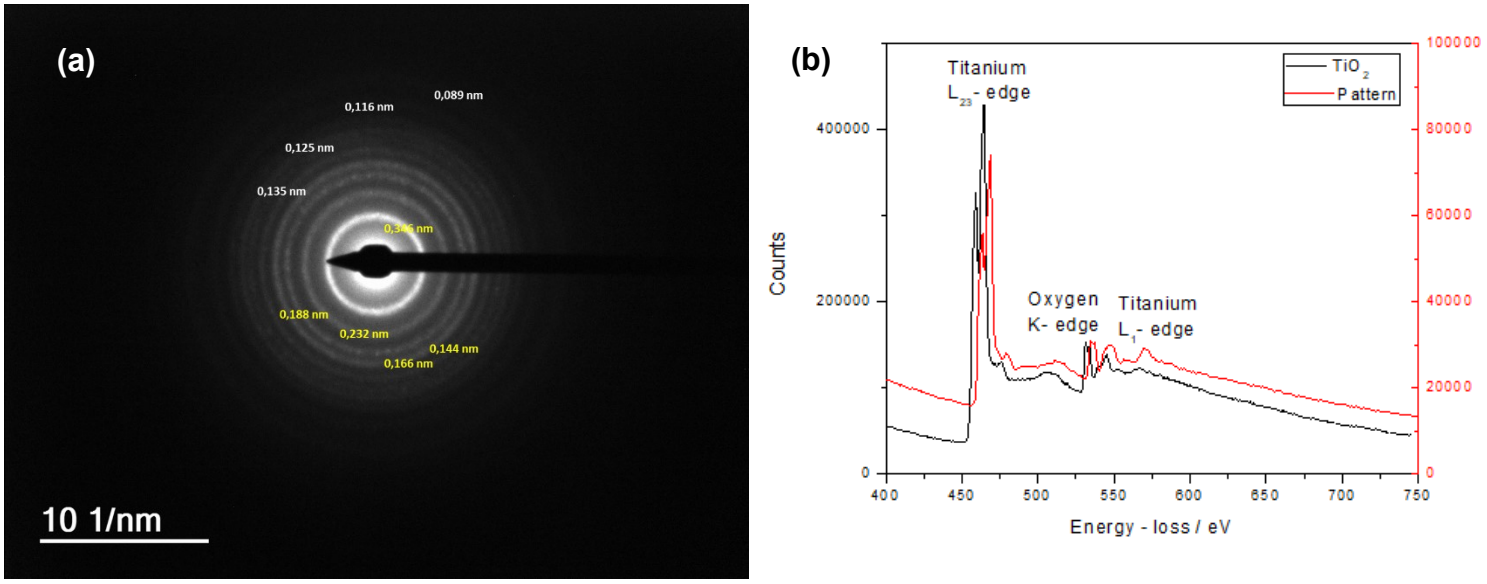

Figure 5: Electron diffraction pattern (a) and EELS spectrum for TiO_2 nanoparticles (b).

2.3.2 Photocatalytic activity of the green TiO_2 in the degradation of methylene blue

The degradation tests with methylene blue dye were run as standard photocatalysis assay to test the effectiveness of the synthesized catalyst. Figure 6-a) shows the evolution of the normalized methylene blue dye concentration as a function of the irradiation time of the UV-C lamp in the absence and presence of the catalyst. The dye presented 82% photolysis after 300 minutes of residence time only under the action of the lamp. In the presence of the catalyst, the degradation was 95% at the same time. In the tests conducted with the catalyst, the system was left for one hour in the dark for measurements of dye adsorption on TiO_2. The adsorption fraction was 54%. The high adsorption potential is probably related to the high specific surface area of the material.

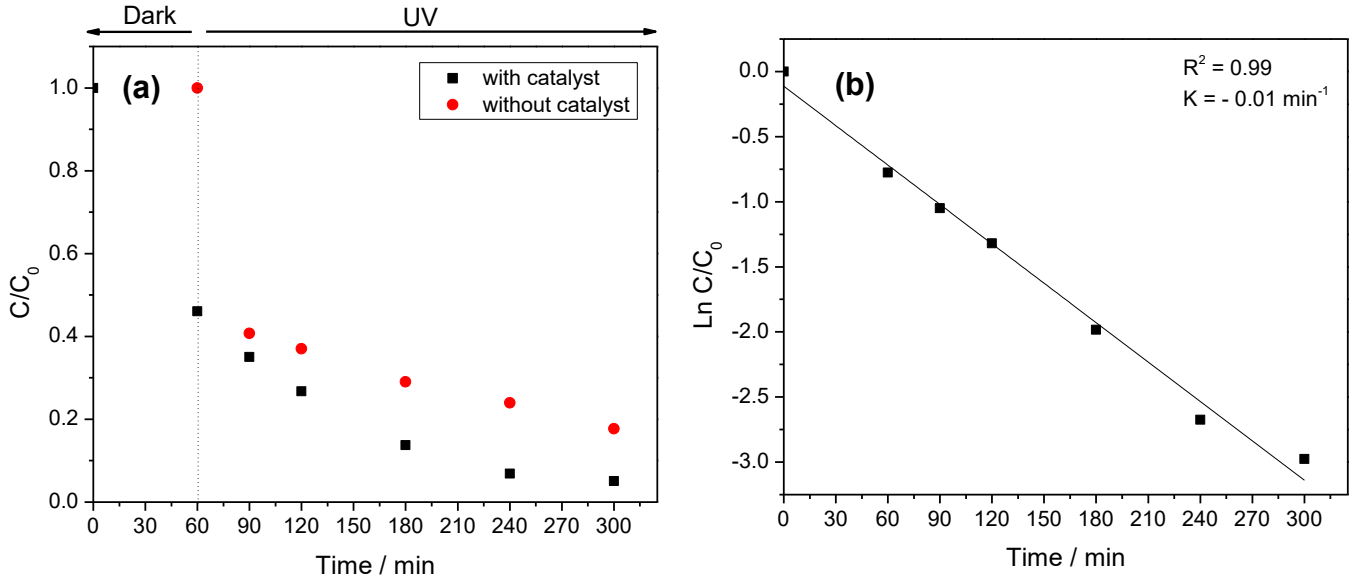

Figure 6: Degradation of the methylene blue dye under UV-C irradiation in the absence and presence of the synthesized TiO_2 catalyst (a) and kinetic model adjustment of dye degradation in the presence of the catalyst (b).

By the analysis of the degradation curve it is possible to note that with the presence of the catalyst the degradation rate is higher, since for equal times the concentration of the dye is lower in the presence of the oxide than without it. In 180 minutes, in the presence of the catalyst, the dye concentration is already lower than that after 300 minutes of the test performed without the catalyst, that is, the same degradation result is achieved in almost half the time with the use of the catalyst.

The degradation efficiency, as can be seen in Figure 6-a), is dependent on the reaction time and the sample to be degraded, and the degradation reaction rate for the methylene blue under the

action of the titanium dioxide catalyst in the presence of UV light is commonly expressed by Equations 8-9 (FRUNZA, *et al.*, 2018):

$$-r = \frac{dC}{dt} = \frac{kKC}{1+KC} \quad \text{Eq. (8)}$$

Where: C is the concentration of methylene blue;
k is the rate constant of the degradation reaction;
K is the adsorption equilibrium constant.

Equation 8 can be simplified:

$$-r = \frac{dC}{dt} \approx kKC \approx k'C \quad \text{Eq. (9)}$$

Where: k' is the apparent rate constant.

This consideration is based on the Langmuir-Hinshelwood model, which assumes that equilibrium of adsorption is established much faster than the reaction. Based on this, Figure 5-b) shows the correlation between lnC and reaction time for the determination of the reaction constant, considering first-order kinetics. The kinetic constant found was k = 0.01 min^{-1}. This value is close to that mentioned by Azeez et. al. (2018), in which the determined reaction constant rate was 0.018 min^{-1} for a catalyst concentration of 100 mg L^{-1} and 10 mg L^{-1} of methylene blue solution. It is noteworthy that each system even due to its geometric characteristics may have different behaviors.

2.3.3 Photocatalytic activity of the green TiO_2 in the degradation of the refinery wastewater MBR permeate

Figure 7 shows the TOC and TN removals achieved by the degradation tests. All the tests were performed at the same time of 90 minutes and at the same concentration of catalyst at the different pH values of 2, 4, 6, 8 and 10. Figure 7 shows higher TOC removal efficiency at pH 8 and 10. A removal of approximately 32% TOC is achieved after 90 minutes of photocatalytic reaction at pHs 8 and 10. This fact is explained by the complexity of the organic compounds in the oil refinery effluents, which can be in the positive, neutral or negative forms (SHAHREZAEI *et al.*, 2012).

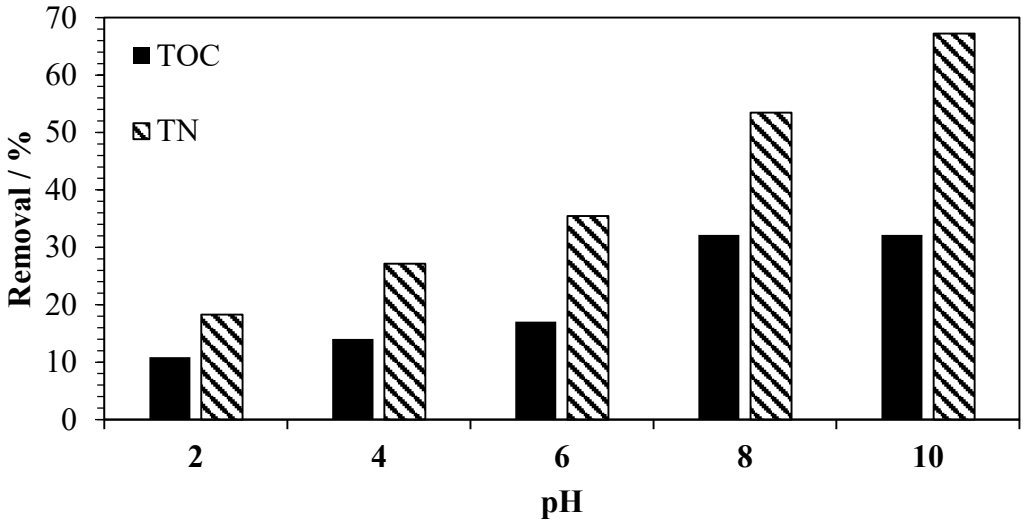

Figure 7: Effect of pH in photodegradation. TOC and TN removals after photodegradation as a function of the pH.

*The raw effluent before the photodegradation tests was at pH 7.08.

The surface of the TiO_2 is amphoteric, that is, it has the characteristics of acid or base according to the pH of the medium. This phenomenon is related to the zero load point (pH_{zpc}) of the catalyst being equal to 6.2 (CHOU and LIAO, 2005). In acid medium (pH<6.2), the catalyst surface is positively charged, while in basic mediums its negatively charged (pH>6.2) and three species are involved at this context: TiO^-, $TiOH_2^+$ and TiOH according to Equations 10-11 (DIYA'UDDEEN, *et al.*, 2011):

$$TiOH + H^+ \longleftrightarrow TiOH^{2+} \text{ at } pH<pH_{zpc} \qquad \text{Eq. (10)}$$

$$TiOH + OH^- \longleftrightarrow TiO^- + H_2O \text{ at } pH>pH_{zpc} \qquad \text{Eq. (11)}$$

In acid media, the predominant oxidative species are the vacancies in the valence band (h^+), while $OH^{\cdot}$ are predominant in basic media because more hydroxyl ions will be available on the TiO_2 surface to be oxidized by raising the photocatalytic potential (AKPAN and HAMEED, 2009).

Due to the results of better performances of TOC removal at alkaline pH, it is inferred that most of the compounds present in the treated effluent have a positive charge favoring the electrostatic attraction between the species and the catalyst and increasing the rate of degradation. It is worth mentioning that the effluent used by the present work underwent a treatment step in a Membrane Bioreactor, that promoted the removal of about 90% of the organic matter from the raw refinery effluent (MOSER, 2017), which can generate different results which regards to

optimized pH conditions when compared to other studies with petroleum refinery effluent whose raw effluent is crude without further treatment.

The compounds removed at that stage by the photocatalytic process are those of difficult degradation, since the biodegradable ones were practically all removed by the MBR. Thus, the removals achieved for the complex matrix effluent whose components are recalcitrant are considerable given the short treatment time (90 minutes).

Shahrezaei *et al.* (2012) found a higher percentage of organic pollutants removal in the primary refinery wastewater at pH 3, while Pakravan *et al.* (2015) noticed an increase in photodegradation by raising the pH from 3 to 6 also in primary refinery wastewater. Ani *et al.* (2018) presents a work in which the degradation of methyl phenyl sulphide was favored in alkaline medium while methyl benzimidazole sulphide was better degraded at neutral pH. As previously stated, the nature of the effluent greatly impacts on the percentage of degradation in the presence of the catalyst and, in particular, the effluent of the present study has undergone a previous treatment.

In relation to total nitrogen (TN), it is observed that with the increase of pH, the greater the removals, and the best percentage of 67% removal was reached in pH 10.

One fraction of nitrogen present in the TN of the oil refinery effluent concerns the ammonia that is generated in the processes of oil treatment, especially when heating the amine groups present in the compounds of its constitution (KENARI *et al*, 2010). The effluent has a loading of phenolic compounds that inhibit nitrification by microorganisms, limiting the efficacy of the biological treatment processes in TN removal besides the small alkalinity of the medium (FIGUEROLA and ERIJMAN, 2010). Therefore, advanced oxidative processes have been reported in the literature as an alternative for the conversion of ammonia and organic nitrogen to nitrogen or nitrate gas in these effluents (CAPODAGLIO *et al.*, 2015), which is corroborated by the data obtained in the present work, on what reduced treatment times (90 minutes) in the presence of the catalyst, practically 70% TN was removed. Ammonia (NH_3) establishes with ammonium ions (NH_4^+) an equilibrium in water which is disadvantageous in the ammonia direction at pHs higher than 8.5-9. So can be concluded that NT removal occurred by the oxidation or adsorption and not by drag.

The results obtained in the present work of a greater removal of TN at alkaline pHs is in agreement with Li *et al.* (2009) who found in their studies a greater removal of ammonia in water under alkaline conditions (pH> 7) using ozone as an oxidizing agent. Chiou *et al.* (2008) *apud* Jing *et al.* (2011) found a more effective degradation of meta-nitrophenol at neutral and slightly alkaline pH. These authors believe that in these conditions of pH, the surface of the catalyst will be mostly in the form of TiO^- and the nitrogenous molecules in their neutral form, favoring interactions of type hydrogen bonding which will aid in the process of adsorption and, consequently, of the degradation.

Osin *et al.* (2018) obtained degradation of 40% of 0.07 mM 4-nitrophenol after 7 hours of photocatalysis using TiO_2 at 500 mg L^{-1}. These results support the potential of the catalyst synthesized in the present work at TN removal from refinery effluents, since in lower concentrations and lower reaction times, higher percentages of removal were obtained.

Figure 8 shows the influence of catalyst concentration on the removal of TOC and TN. It is observed that the higher the catalyst concentration, the smaller the TOC and TN removals. The concentration of 100 mg L^{-1} was the one with the best percentages of removal, 32% of TOC and 67% of TN, evidencing that it was the optimum concentration among the tested, from which there was a decrease in catalyst activity. Saien and Nejati (2007) also found the concentration of 100 mg L^{-1} as the most efficient in the removal of COD from the refinery effluent. The same value was obtained by Shahrezaei *et al.* (2012). These results are in agreement with the findings of several other authors, according to which, above certain concentrations of catalyst, there was decrease in the removal of TOC (TOPARE *et al.*, 2015). Khan *et al.* (2015) found that at TiO_2 concentrations above 1.2 g L^{-1} the process efficiency decreased. The same was reported by Ling *et al.* (2015) in the treatment of phenol at concentrations higher than 1 g L^{-1} of the catalyst, the degradation efficiency decreased.

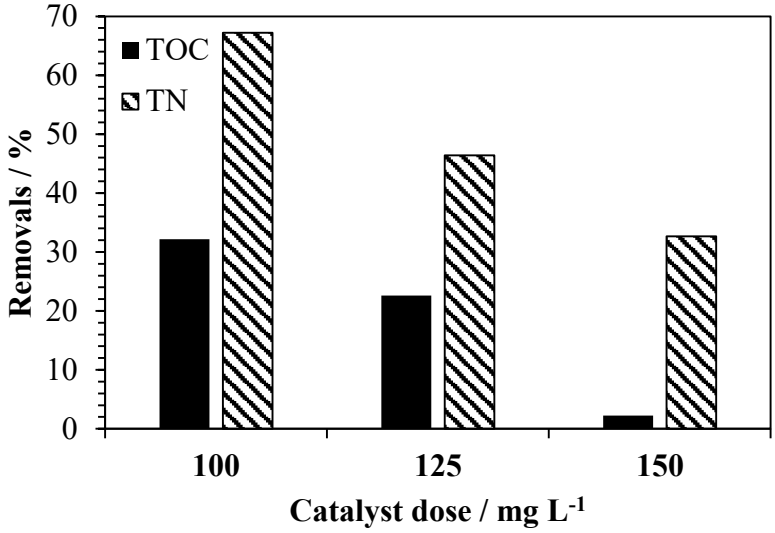

Figure 8: Effect of catalyst concentration in photodegradation. TOC and TN removal values after photodegradation as a function of TiO_2 catalyst dose.

Some authors point out that there is a linear relationship between the catalyst mass and the initial reaction rates (JAIN and SHRIVASTAVA, 2008; AKPAN and HAMEED, 2009). High catalyst concentrations imply a greater number of active sites available. However, an increase in catalyst concentration above a certain limit does not mean a change in degradation efficiency, and may reduce it (PATIL *et al.*, 2012). The explanation is that at higher concentrations of the catalyst, the increased turbidity of the solution may reduce the penetration of light and cause its scattering. In addition, the agglomeration of the catalyst can occur at higher concentrations promoting the reduction of the active sites and consequently compromising the efficiency (ANI *et al.*, 2018).

In general, the composition of the refinery effluent is very complex and may contain different types of organic pollutants. Because it is a study with real effluent, the obtained percentage values of degradation are in agreement with other authors, as Khan *et al.* (2015), whose study on the degradation of the real refinery effluent using commercial TiO_2 obtained degradation results in terms of COD ranging from 25.35% to 40.68% when changing parameters such as pH and catalyst dosage.

The Spearman rank correlation analysis indicated significantly positive correlations between pH and TOC removal ($r = 0.9747$, $p = 0.005$) and between pH and TN removal ($r = 1$). The opposite behavior was observed in the correlations between catalyst dose and TOC and TN removal (both $r = -1$), inversely related. Based on these results and anchored in the earlier discussed, can be inferred that the two parameter analyzed consistently influence the organic

matter removal and catalyst dose parameter has a stronger relation with the removal of the studied variables.

The kinetic study of TOC removal in the presence of TiO_2 catalyst revealed that the first order kinetic model fitted very well the data with a correlation coefficient (R^2) equal to 0.96 being adequate to describe the mechanism (Fig. 9). Thus, the figure of merit EE_0 can be used to determine the energy expenditure in each one of the conditions tested. Table 2 summarizes the EE_0 values and as can be seen, higher pHs promotes a less energy consumption to remove an order of TOC. Regarding the catalyst dose, a more efficient utilization of photons occurs in the lowest concentration. This is an interesting result, especially when thinking about the reactor scale-up. Lower catalyst dose besides propitiating savings in the purchase of reagent, provides less energy consumption. The EE_0 result in the best condition evaluated (pH = 10 and catalyst concentration = 100 mg L^{-1}) is 3.38 times lower than that in the worst condition of pH removal (pH = 2) and 20.40 times smaller than in the worst catalyst concentration (150 mg L^{-1}). This result corroborates the statistical test that showed a higher correlation and, therefore, a higher sensibility among the catalyst dose and the TOC removal.

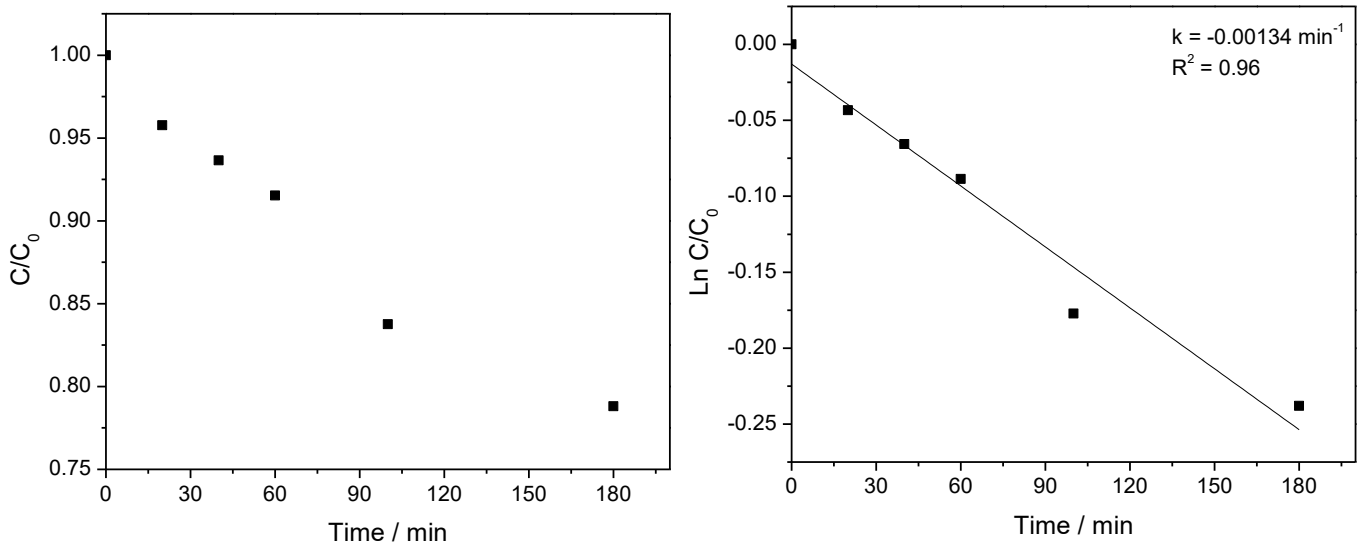

Figure 9: TOC removal under UV-C irradiation in the presence of the synthesized TiO_2 catalyst (a) and first order kinetic model adjustment of TOC removal in the presence of the catalyst (b) at concentration of 100 mg L^{-1} and medium pH = 10.

Table 2: Electrical Energy per Order (EE_0) for TOC removal in the evaluated tests varying pH between 2-10 and catalyst concentration from 100 mg L^{-1} to 150 mg L^{-1}.

Evaluated Parameter	Value	EE_0 (KWh m^{-3}.order^{-1})
pH	2	1203.61
	4	914.18

Evaluated Parameter	Value	EE_0 (KWh m^{-3}.$order^{-1}$)
pH	6	737.74
	8	356.29
	10	356.29
Catalyst concentration	100 mg L^{-1}	356.29
	125 mg L^{-1}	830.53
	150 mg L^{-1}	7267.22

To determine the possibility of reuse and recycle of the catalyst in the photocatalysis under UV irradiation, the degradation tests in the best condition found (100 mg L^{-1}, pH = 10) were performed several times and the data obtained are shown in Figure 9. At each repetition, the catalyst was washed with distilled water and filtrated by membrane. The results indicate a certain stability of the photocatalyst being possible to use it at least 4 times. It suggests that although there is contribution of the adsorption for the TOC removal, the low loss of performance with the catalyst reuse indicates that with the photocatalytic activity the oxidation of the adsorbed materials occurs releasing active sites.

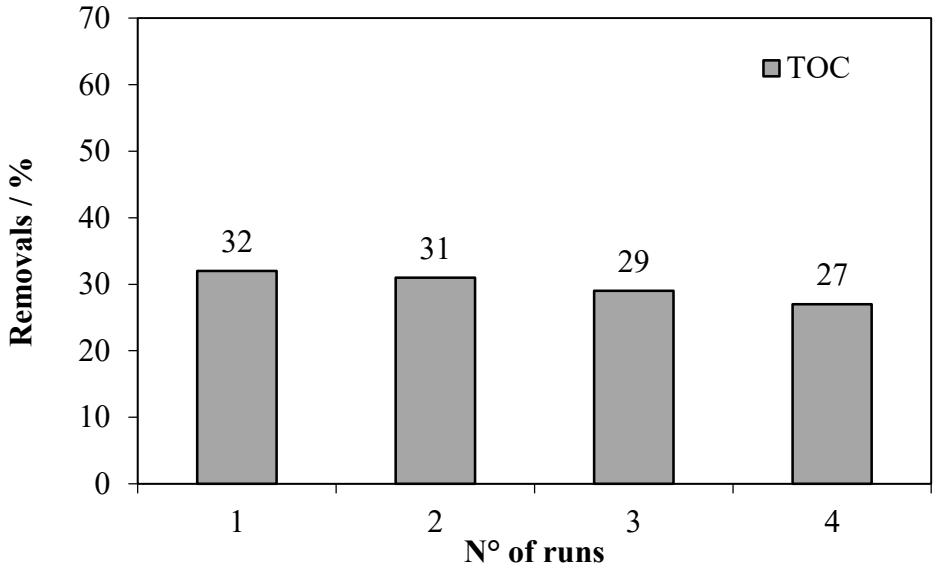

Figure 10: Reusability of the catalyst for petroleum refinery wastewater degradation.

2.4 CONCLUSION

Nanoparticles of pure titanium dioxide in the anatase phase with a mean crystallite size of 14 nm were obtained by environmentally friendly microwave assisted route under mild conditions, with low consumption of chemical reagents and reduced reaction time. They were efficient in the degradation of organic molecules, according to standard test carried out with methylene blue, in which 95% degradation was achieved in 300 minutes of reaction in the presence of

UV-C light (254 nm). The synthesized material was also promising in the treatment of petroleum refinery wastewater, since under the best condition tested and in a relatively low reaction time of 90 minutes, it removed 32% TOC from the effluent and 67% TN in pH equal to 10 and catalyst dose of 100 mg L^{-1}. At more acidic pHs, lower degradations were obtained evidencing that the effluent post ultrafiltration in the Membrane Bioreactor presents compounds that are oriented positively in alkaline media favoring the adsorptive process in the catalyst and, consequent degradation. Best dosing of the catalyst for treatment reveals a relatively low concentration of the material, which facilitates its large-scale implementation. It was observed that higher values of TiO_2 concentration negatively affect the degradation efficiency. These results support the fact that pH and catalyst dose are extremely important parameters that affect catalyst photoactivity, as confirmed by the Spearman's correlation rank. The Electrical Energy per Order (EE_0) varies between 356.29 KWh m^{-3} $order^{-1}$ (pH = 10) and 1203.61 KWh m^{-3} $order^{-1}$ (pH = 2) among the pHs tested and between 356.29 KWh m^{-3}.$order^{-1}$ and 7267.22 KWh m^{-3} $order^{-1}$ when varying the catalyst dose, 100 mg L^{-1} and 150 mg L^{-1}, respectively. So, besides the better condition for TOC and TN removal, the catalyst dose equal to 100 mg.L^{-1} and the reactional medium pH equal to 10 is the better condition from an energy use point of view. The catalyst was shown to be stable for reuse at least four times. The results showed that TiO_2 is a promising tool in the removal of recalcitrant compounds of difficult degradation in the refinery effluent and can bring benefits if used in a step before the polishing processes with a view to reuse. Thus, it is suggested that other studies can be conducted to evaluate alternatives for catalyst retention as new membranes and additives that increase the percentage of degradation of the pollutants.

CHAPTER 3

Potential use of green TiO_2 and recycled membrane in a Photocatalytic Membrane Reactor for oil refinery wastewater polishing

3.1 INTRODUCTION

In the oil refining processes, an average of 0.7 to 1.2 m^3 of water per 1 m^3 of crude oil is used, which generates a quantity of wastewater of 0.3 to 1.4 times the volume of the processed oil (IPIECA, 2010; MESQUITA *et al*., 2018). The transformation of the raw material leads to a series of products such as gasoline, naphtha, kerosene, diesel, lubricating oil, and various solvents, which can generate toxic effluents (phenolic compounds, sulphides, ammonia, cyanides, and polyaromatic and aliphatic hydrocarbons) for aquatic and terrestrial biotas, some of which are even carcinogenic to several organisms (JAMALY *et al*., 2015). Therefore, advanced treatments that enable wastewater reclamation are desired (ANI *et al*., 2018).

Membrane bioreactors (MBRs) have been successfully used for oil refinery wastewater treatments (MOSER *et al*., 2019). However, a polishing treatment of the MBR permeate is required to remove the inorganic and recalcitrant organic compounds to attain water reclamation. Generally, reverse osmosis (RO), nanofiltration (NF), electrodialysis, and ion exchange have been used for refinery wastewater desalting. However, nonbiodegradable compounds and associated biological metabolic products originating from the biological process such as soluble microbial products (SMPs) and extracellular polymeric substances (EPSs) cause fouling in membranes and resins, which negatively impacts the salt removal processes and increases the operational costs (MOSER *et al*., 2019). In addition, these compounds compromise the treatment of the membrane concentrate from the desalting processes, owing to their inhibitory effect on the crystallisation (ZHAO *et al*., 2013; MOSER *et al*., 2017), and even may lead to the generation of cytotoxic compounds such as trihalomethanes in disinfection stages with chlorine (MOSER *et al*., 2018).

In this regard, the removal of residual organic matter of the refinery wastewater is necessary prior to the polishing processes. Photocatalytic membrane reactors (PMRs) are promising alternatives for the removal of the recalcitrant compounds. This technology combines photocatalytic oxidation with membrane filtration (LEONG *et al*., 2014; MOLINARI *et al*., 2017; MOZIA, 2010). The PMRs are considered a green technology because they increase the potential of each process, creating a synergistic effect with consequent reductions in environmental and economic impacts. The membranes enable continuous operations with the retention/recuperation of the catalyst and separation of the reaction products as soon as they are generated, which provides the displacement of the equilibrium in the direct and desired direction of the reaction. They also enable the control of the residence time of the pollutants

and their intermediate degradation compounds, guaranteeing the expected mineralisation (LEONG *et al*., 2014).

On the other hand, the catalyst in a PMR could minimise the membrane fouling, which is one of the largest problems in membrane operations. The catalyst in the PMR promotes the pollutant degradation reducing the formation of the cake layer (ZHANG *et al*., 2018). The titanium dioxide (TiO_2) catalyst is one of the most studied catalysts. Electron–hole pairs, which migrate to the surface of the oxide, are generated upon its irradiation by ultraviolet (UV) light. Therefore, they act as redox species producing radicals, which can react with organic pollutants (LAI *et al*., 2015; ABDEL-MAKSOUD *et al*., 2018).

PMRs can be constructed by two different approaches. The first approach is based on TiO_2 in the form of a nanoparticulate powder suspended in the reaction mixture followed by a membrane unit (slurry PMR). The second approach is based on TiO_2 immobilised on the membrane. The first configuration has some advantages over the second configuration (HATAT-FRAILE *et al*., 2017; MOZIA, 2010). For example, the active surface area of the suspended catalyst is larger, which provides larger efficiencies in the degradation of the pollutants. In addition, the amount of used catalyst may be adjusted according to the characteristic of the effluent to be treated. When the catalyst is immobilised on the membrane surface, the membrane is subject to degradation by the incident UV light. The membrane degradation by the incident UV light can be avoided in the slurry PMR configuration by separating the reaction and filtration processes in two separate compartments (ZHANG *et al*., 2016).

According to Padaki *et al*. (2015), PMRs constitute a new and promising technology for the treatment of wastewaters containing oils, particularly refinery oils. They enable the degradation of hydrocarbons and other toxic compounds and thus contribute to the purification of the effluent and its potential reuse. Moslehyani *et al*. (2015) developed a PMR using a commercial TiO_2 (P25) and ultrafiltration (UF) membrane for the treatment of synthetic oil refinery wastewater with a concentration of grease and oil of 100 mg L^{-1}. They achieved 90% degradation of the pollutants by the photocatalytic process and their removal after passage through the membrane, besides the retention of 99% of the catalyst by the membrane.

The PMRs are characterized by the concept of process intensification, which is defined as any chemical engineering development leading to cleaner, more compact, and more energy efficient

technologies (IGLESIAS *et al*., 2016). Thus, they constitute an advanced technology, which meets the current demands for cleaner production and treatment routes with lower environmental impacts (VAIANO *et al*., 2015). The system can be further improved, in terms of pollution reduction, by the use of catalysts synthesised by green routes as well as the reuse or recycling of membranes, such as the end-of-life RO membrane.

RO membranes have been widely used, in desalination processes for potable use and in the polishing step for the generation of reuse water. However, although their use is increased, the disposal of these membranes in landfills is also increased; their lifetimes are in the range of five to seven years (LAWLER *et al*., 2015; ZIOLKOWSKA, 2015). The recycling of end-of-life RO membranes through chemical oxidation with sodium hypochlorite for use in microfiltration (MF) and UF processes is a feasible alternative to reduce the impact of the disposal of these modules (COUTINHO DE PAULA and SANTOS AMARAL, 2018; GARCÍA-PACHECO *et al*., 2018) and investment and operational costs of the PMR.

The development of the system with catalysts synthesised by cleaner routes and use of recycled membranes in the PMR provide a larger sustainability of the technology. Several methods are used for the preparation of the TiO_2 catalyst such as the sol–gel, chemical vapour deposition, and hydrothermal methods (GUO *et al*., 2012; REINKE *et al*., 2015; MOHAMED *et al*., 2017). These methods typically involve long complex procedures at high temperatures (CORRADI *et al*., 2005; NOMAN *et al*., 2018). The recent use of microwave radiation in the synthesis of this material was quite efficient, as it led to a rapid heating and reduced reaction time, energy consumption, and processing costs, in addition to the larger uniformity of the product (NIU *et al*., 2014; FILIPPO *et al*., 2015; FALK *et al*, 2018). Thus, the use of a microwave-assisted synthesised catalyst with a low reagent consumption is a promising alternative to PMRs.

In this study, the potential of coupling a PMR comprising a recycled RO membrane and green TiO_2 nanoparticles with an MBR for the treatment of oil refinery wastewater was investigated. The removal of recalcitrant compounds by the system was evaluated. The photocatalytic stability of the green TiO_2 and membrane chemical stability were also investigated in consecutive reaction cycles. Several studies involving the use of PMRs in the treatment or degradation of synthetic compounds or single matrices have been reported. However, few studies considered real effluents and no study involving real refinery wastewater treated by a

catalyst synthesised through a cleaner route in a PMR has been reported. The use of a recycled membrane in a PMR is also novel.

3.2 MATERIALS AND METHODS

3.2.1 Oil refinery wastewater

The refinery wastewater was collected in a Brazilian oil refinery after a primary treatment for oil removal by an American Petroleum Institute (API) separator and dissolved air flotation. After the primary treatment, the wastewater was treated in a bench-scale MBR.

3.2.2 Membrane Bioreactor

The MBR comprised a 3.36-L (effective volume) biological reactor, in which a hollow fiber UF membrane (ZeeWeed 1 – GEPVDF, average pore diameter: 0.04 μm, area: 0.047 m^2) was submerged. An air diffuser with a flow rate of 0.5 $Nm^3\ h^{-1}$ was installed at the bottom of the membrane module to supply oxygen for microorganisms and prevent membrane fouling. The biological sludge concentration was maintained at approximately 3.7 g L^{-1}, while the pH was adjusted to approximately 7.0. The average food-to-microorganism ratio and organic loading rate were maintained at 0.66 kg chemical oxygen demand (COD) kg^{-1} mixed liquor suspended solid (MLSS) d^{-1} and 2.44 kg COD $m^{-3}\ d^{-1}$, respectively. The MBR was operated at a hydraulic retention time of 6 h and sludge retention time of 45 days. The UF permeate flow rate was maintained at 0.55 L h^{-1}.

The MBR permeate was used as a feed for the photodegradation tests in the PMR. It was stored in a refrigerator at 4 °C to avoid changes in characteristics. Table 3 shows the main physicochemical characteristics of the permeate.

Table 3: Main physicochemical characteristics of the UF permeate from MBR treating refinery wastewater.

Parameter	Unit	Mean ± Standard Deviation
COD	$mgO_2\ L^{-1}$	45.4 ± 24.8
DOC	mg L^{-1}	15.4 ± 8.7
IC	mg L^{-1}	6.7 ± 2.2
Alkalinity	mg L^{-1} $CaCO_3$	31.4 ± 31.9
Chloride	mg L^{-1}	598.0 ± 167.9

Parameter	Unit	Mean ± Standard Deviation
Sulfate	mg L^{-1}	198.6 ± 31.1
Ammonia	mg L^{-1}	0.9 ± 0.7
Total Nitrogen TN	mg L^{-1}	36.2 ± 4.9
Conductivity	µS cm^{-1}	2393.1 ± 486.4
Color	PtCo L^{-1}	44.2 ± 16.8
Turbidity	NTU	0.77 ± 0.11

DOC: dissolved organic carbon; IC: inorganic carbon

3.2.3 Green TiO_2 synthesis

The catalyst was synthesised based on the study by Li and Zeng (2011) using a modified route with a reduced use of chemical reagents and microwave irradiation. First, 6 mL of titanium tetrachloride ($TiCl_4$, Merck) was added in 150 mL of distilled water in a round-bottom flask immersed in an ice bath. Subsequently, 10 mL of ammonium hydroxide (NH_4OH, Sigma-Aldrich) was added to the mixture to adjust the pH to 8. The system was allowed to stir in the bath for 30 min. Subsequently, the reaction mixture was placed in a microwave oven (Milestone Start D) and subjected to a heating ramp to 80 °C for 6 min. This temperature was then maintained for 4 min. Subsequently, another cooling ramp was carried out to 50 °C for 20 min. The obtained material was washed with water and centrifuged at 3500 rpm several times until neutral pH was achieved. It was then kept in a kiln for drying at 85 °C for 2 h and calcined at 400 °C according to a programmed heating ramp of 25 °C to 400 °C in 1 hour and 15 minutes, kept in 400 °C for 2 hours and finally 400 °C to 25 °C in 1 hour.

3.2.4 Recycled Membranes

The recycling technique was based on the chemical oxidation of a thin-film-composite RO membrane, proposed by De Paula et al. (2017). The membrane was immersed in a commercial sodium hypochlorite bath (contact intensity: ~300000 parts per million h) at room temperature. The end-of-life membrane sample used in this study was withdrawn from a spiral module (FilmTec BW30, diameter: 2.0×10^{-1} m, length: 1.0 m, active area: 41 ± 3 m^2). This membrane was used in a pilot plant for the polishing of the oil refinery effluent treated by the MBR. The

new BW30 membrane exhibited a permeability of 3.0 L h^{-1} m^{-2} bar $^{-1}$ and NaCl (2.0 g L^{-1}) rejection of 99.5% (DOW, 2012).

3.2.5 Photocatalytic Membrane Reactor

3.2.5.1 Experimental setup

The PMR consisted of a cylindrical PurePro Ultraviolet water steriliser reactor (50.5 × 320 mm^2; capacity: 280 mL) with a quartz tube, where a low-pressure mercury vapour lamp (radiation of 6 W at 254 nm) was connected; rectangular membrane module (effective permeation area of 7 × 17 cm^2 = 119 cm^2), where the recycled membrane was placed; diaphragm pump (Flojet D2235); rotameter used to verify the circulation flow; pressure gauge; needle valve for pressure control; and digital thermometer used to monitor the feed temperature (Figure 11).

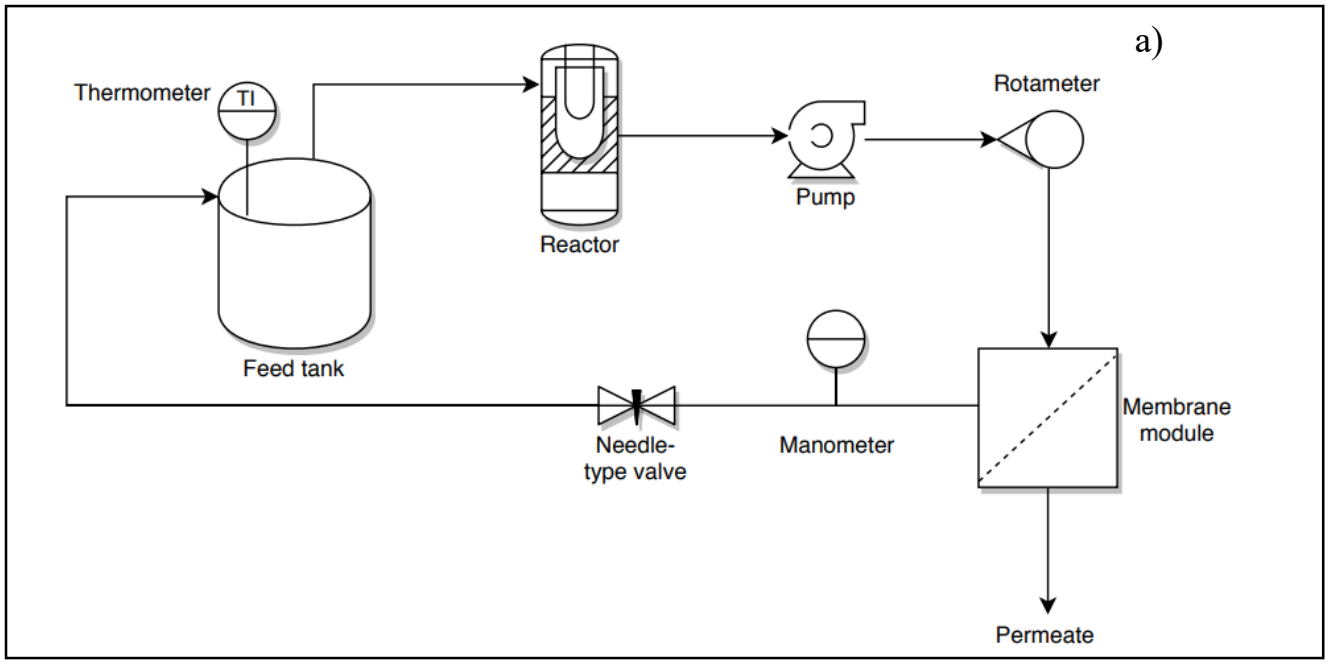

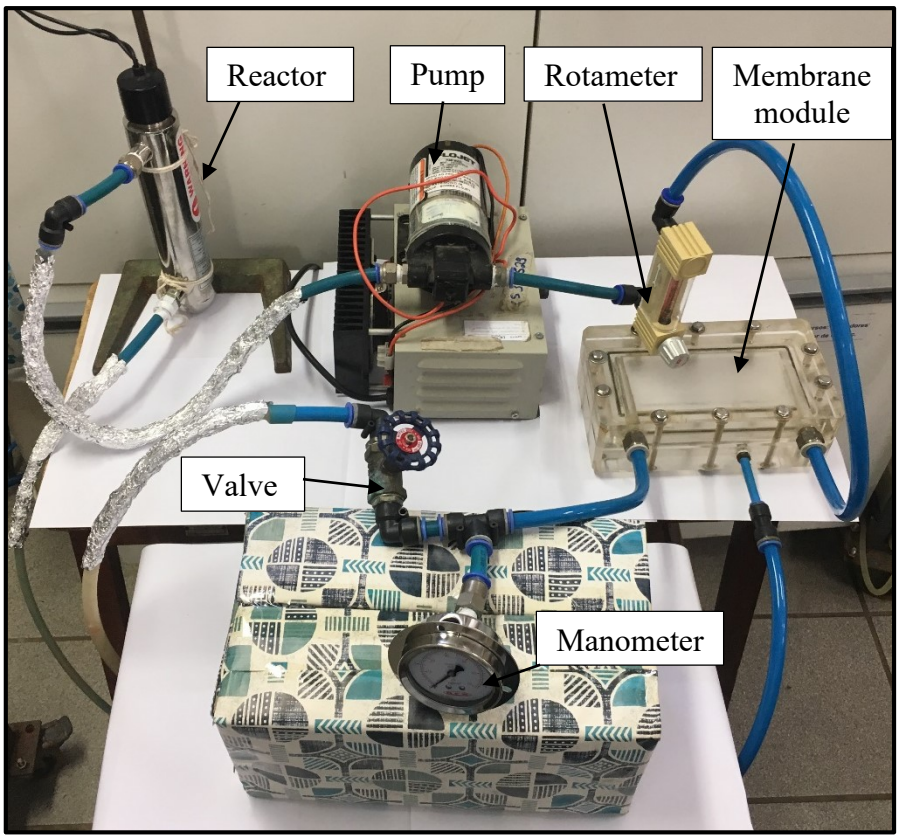

Figure 11: PMR's schematic diagram (a) and top view (b).

3.2.5.2 Experimental procedure

The feed tank was filled with 1 to 3 L of MBR permeate (the pH was adjusted to 10 with a 0.1 mol L-1 NaOH solution (Dinâmica)) and 125 mg L^{-1} of green TiO_2 according to the previous studies. The feed temperature was maintained at 21 ± 2 °C. The system was operated in the batch mode by recirculating the feed through the UV reactor and membrane module. The recycled membrane module was operated at a pressure of 1 bar and feed flow rate of 44 ± 2 L h^{-1}. The recycled membrane was compacted with ultrapure water filtration. The operation times of the tests were in the range of 20 to 320 min. Samples were collected at predetermined times to evaluate the PMR performances. The permeate flux was monitored after every 5 min to verify the membrane fouling as well as the changes in properties of the selective layer due to the activity of the catalyst and formed oxidising byproduct. Tests with a commercial catalyst (P25 Degussa, Evonik) were also carried out for comparison to the synthesised material. Tests only with the permeation of the wastewater through the membrane, only with photolysis by UV light bypassing the membrane, and in the darkness bypassing the membrane (adsorption verification)

were performed to verify the individual contributions of these processes to the COD removal from the wastewater.

3.2.6 Calculation

Flux normalization to 25 °C was carried out using a correction factor related to the fluid viscosity as shown in Equation 12:

$$J_N = \frac{\Delta V}{A.\Delta t} \cdot \frac{\mu(T)}{\mu(25°C)} \quad \text{(Eq. 12)}$$

where J_N is the normalized permeate flux at 25 °C, $\Delta V/\Delta t$ is the permeate volume by time, A is the permeation area, μ(T) is the water viscosity at the process temperature, and μ(25 °C) is the water viscosity at the temperature at 25 °C.
The flux decline (FD) was measured by means of the equation 13:

$$FD = \left(1 - \frac{J}{J_0}\right) x100 \quad \text{(Eq. 13)}$$

Where J is the normalized flux at the end steady state of the tests developed with the effluent and J_0 is the normalized flux at the beginning of the same experiments.

The water permeability at 25 °C were obtained from the slope of the linear regression of the pressure versus normalized flux data of distilled water in the recycled membrane at pressures of 2.5, 2, 1.5, 1 and 0.5 bar. Based on the calculated water permeability, the intrinsic membrane resistance to filtration was calculated according to equation 14:

$$R_m = \frac{1}{K.\mu(25°C)} \quad \text{(Eq. 14)}$$

Where R_m is the intrinsic membrane resistance, K is the water permeability and μ(25 °C) is the water viscosity at the temperature at 25 °C.

The total fouling resistance were calculated based on the resistance in series concept (Eq. 15). At this concept, the total resistance (R_t) comprises the intrinsic membrane resistance (R_m) and fouling resistance R_f.

$$R_t = R_m + R_f \quad \text{(Eq. 15)}$$

The total resistance was calculated according to equation 16:

$$R_t = \frac{\Delta P}{J_N . \mu(25°C)} \quad \text{(Eq. 16)}$$

where ΔP is the applied transmembrane pressure (1 bar) and J_N is the normalised permeate flux at the end of the experiment performed under the operation of the whole system including the catalyst in the feed tank and only permeation at the membrane in the system without catalyst. By subtracting the intrinsic membrane resistance from the total resistance in each test, the fouling resistance was determined in the presence or absence of the catalyst.

The percentage of COD removal was calculated according to Equation 17:

$$R\% = \frac{COD_0 - COD_f}{COD_0} x100 \quad \text{(Eq. 17)}$$

Where: $R\%$ is the percentage COD removal

COD_0 is the initial COD

COD_f is the final COD

The absorbance at 254 nm (ABS_{254}) and TN removal were calculated using equations analogous to Equation 6.

3.2.7 Analytical methods

The MBR permeate and wastewater treated in the PMR were characterised by their pH (Qualxtron QX 1500 pHmeter), conductivity (Hanna conductivity meter), COD (5220B), and TN (D8083) values in accordance with the Standard Methods for the Examination of Water and Wastewater (APHA, 2012) to evaluate the pollutant removal by the system. The TN was measured using a Shimadzu TOC-VCPH analyser.

The luminous intensity of the mercury vapour lamp (5.5×10^{-5} Einstein min^{-1}) was determined by an actinometric test using potassium ferrioxalate reagent (Murov, 1973).

The concentrations of the solutions in the actinometric test were measured using a UV–visible PerkinElmer spectrophotometer (Lambda XL) through calibration curves. The readings of the ABS_{254} values of the samples were performed before and after the treatment in the same equipment to evaluate the removal of aromatic rings from the wastewater.

The particle size distribution of the catalyst was measured using an LA-950 high-performance laser diffraction particle size analyser (Horiba, Japan). The sample was dispersed in Milli Q ultrapure water.

The morphologies of the membranes before and after the tests in the PMR and those of the permeate were analysed using a double-beam microscope (FEI Quanta 3D FEG) equipped with an energy-dispersive spectroscopy (EDS) system. Different samples of the membrane before the process were dried naturally at room temperature, while those after the process in the PMR were washed only with water and allowed to dry at room temperature. All samples were fixed on a carbon tape. The permeate was dried at 110 °C in a kiln. The dry material was dispersed in isopropanol and fixed on a silicon wafer. Before the analysis, all samples were plated with gold–palladium. The membrane was also evaluated by thermogravimetric analysis (TGA; Shimadzu DTG 60-H) at a heating rate of 10 °C min^{-1} in the range of 33 to 1000 °C in a nitrogen atmosphere at a gas flow rate of 50 mL min^{-1}.

To investigate the modifications in the wastewater after the treatment in the PMR, attenuated total reflection Fourier-transform infrared (ATR-FTIR) spectra of the dried MBR permeate after the PMR treatment, pristine membrane, and fouled membrane after the physical cleaning were recorded using a FTIR Shimadzu IRAffinity-1 instrument. For the experiment, 30 mL of the sample after 80 min of treatment was dried in a kiln at 110 °C for 24 h. The dry solid sample was analysed by direct exposure to radiation in the ATR module in the range of 400 to 4000 cm^{-1}.

The toxicities of the MBR permeates after the PMR, UV (only), and membrane (only) treatments were evaluated using the marine species *Aliivibrio fischeri* and Microtox® (Model M500) analyser. The inhibition of *Aliivibrio fischeri* was measured in accordance to the Microtox® standard method for a 81.9% basic test. The tested dilutions of each sample had concentrations of 0, 0.27, 0.55, 1.11, 2.22, 4.44, 11.11, 24.44, 48.88, and 100% v/v. The effective concentration (EC50) (concentration of the sample that corresponds to 50% inhibition of bacterial luminescence) was calculated after 30 min of contact.

3.2.8 Statistical analysis

Kruskal-Wallis non-parametric test for multiple independent samples, Wilcoxon's T test for two dependent samples, and Mann-Whitney U-test for two independent samples were performed between flux values and COD and ABS_{254} removals obtained in order to detect statistically

different differences between values. Statistical analyzes were performed by Statistica 10.0 Software.

3.3 RESULTS AND DISCUSSION

3.3.1 Main characteristics of the green catalyst and recycled membrane

The green synthesis route yielded a nanoparticulate TiO_2 with a mean crystallite size of 14 nm and single anatase phase. The material dispersed in water exhibited a bimodal granulometric distribution with average particle sizes of 23 and 743 μm. A more detailed characterisation of the catalyst can be found in Oliveira *et al.* (2019).

The scanning electron microscopy (SEM) image of the pristine membrane (Fig. 12 – a-b) shows an apparently smooth structure having few contrasts, which indicates a topography without considerable variations (DE PAULA et al., 2017; ZHOU et al., 2014). This is expected as the end-of-life RO membrane has undergone chemical oxidation with sodium hypochlorite, in which the aromatic polyamide layer has been removed. In order words, after the recycling, the selective layer was degraded, which yielded the most homogeneous topography in the image (DE PAULA et al., 2017). Typically, a thin-film-composite RO membrane has such selective layer formed under a polysulfone layer by interfacial polymerisation (DONOSE et al., 2013). This process generates a structure having ridges and valleys, which appear as contrasts in the SEM image and indicate a rough surface. Regarding the applicability in the PMR, a smoother membrane surface is beneficial, as it is less prone to fouling than the rough surface (DU et al., 2015). At an increased magnification (Fig. 12-b), fairly irregular regions with various dimensions were observed, some of which resembled sponge- and asymmetric finger-like pores. This structure exhibited similar pore characteristics to those of UF and MF membranes (MOZIA et al., 2015).

The recycled membrane exhibited a permeability of 86 ± 11.4 L h^{-1} m^{-2} bar^{-1}, salt rejection (NaCl 2.0 g L^{-1}) of 16.7 ± 2.5%, contact angle of 75.5 ± 1.7°, and root-mean-square roughness of 6.13 ± 0.86 nm. The increased permeability and reduced saline rejection are associated with the changes in the membrane selective layer by the degradation of the aromatic polyamide layer.

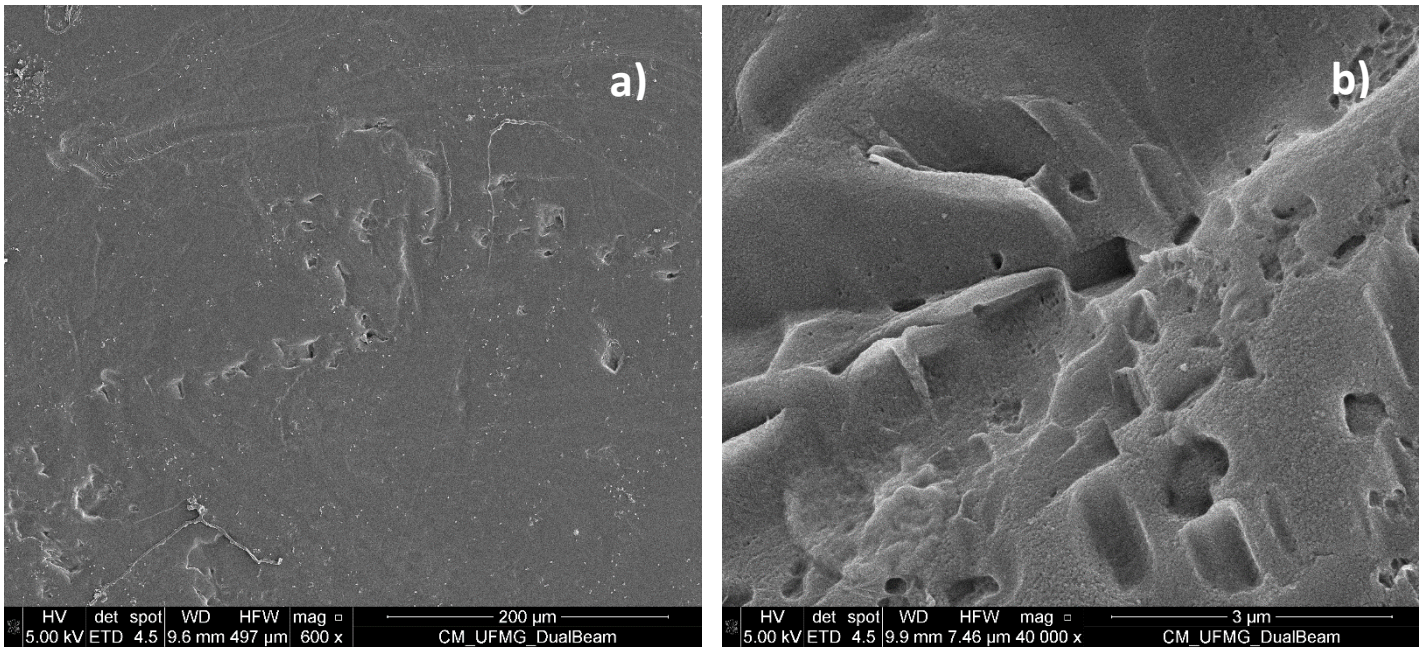

Figure 12: SEM micrographs of different regions and different magnifications of the recycled membrane before the tests in the PMR.

3.3.2 Pollutant removal efficiency in the PMR

The pollutant removal performance of the green TiO_2 in the PMR was compared to that of the commercial TiO_2 catalyst (Figure 13). The PMR operating with the green TiO_2 catalyst exhibited a high pollutant removal efficiency with a COD removal of 56% after 40 min of operation. The PMR operating with the green TiO_2 catalyst could also effectively decrease ABS_{254}, which is indicative of the amount of the most complex forms of organic matter in the sample. A higher value implies that more hydrophobic molecules constitute the effluent. The selected wavelength is associated with the absorption peak of the aromatic rings, including double or triple bonds. Some constituents of this class of compounds are present in the refinery effluent, including polyaromatic hydrocarbons, benzene, toluene, xylene, and several phenols. These constituents are detrimental to the desalination of the wastewater for reuse, because they can contribute to RO and NF membrane fouling (ABDELWAHAB et al., 2009; ESTRADA-ARRIAGA et al, 2016; RUEDA-MÁRQUEZ et al., 2016). The decrease in ABS_{254} is indicative of aromatic ring openings and consequent removals or structural modifications of these compounds (JANSSENS et al., 2017; LIU et al., 2014). The performance of the green TiO_2 in the removal of the aromatic compounds was statistically superior to that of the commercial catalyst, according to the Mann–Whitney *U*-test ($p = 0.030384 < 0.05$). A reduction in ABS_{254} of 54% was achieved after a residence time of 80 min.

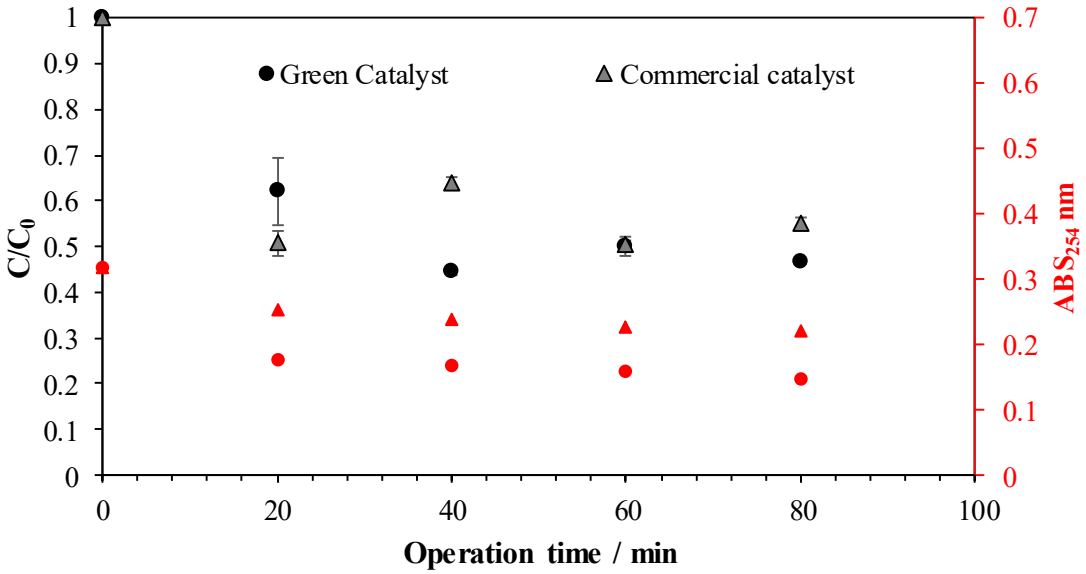

Figure 13: COD removal and Absorbance reduction at 254 nm over time in PMR operating with green catalyst and commercial catalyst.

Unlike the commercial catalyst, which is a mixture of the anatase and rutile phases (HO *et al*., 2009), the synthesised green catalyst exhibited a single phase (anatase), which may be one of the factors that contributed to the differences in performances. The results are valuable considering that the MBR-treated compounds are recalcitrant (NOGUEIRA *et al*., 2016). At a low concentration of the catalyst and reduced residence time (40 min), more than half of the organic load was removed. The petroleum refinery wastewater is a complex matrix consisting of oils, greases, sulphur, nitrogenous, aromatic compounds, etc. The MBR can substantially reduce the contents of many of these organic compounds. However, more complex fractions are not removed during the biological process and may remain in the permeate (LIANG *et al.,* 2004). In addition, microbial byproducts are generated in the biological process (SMP and EPS), which are major fouling agents, reducing the flow in membrane reuse processes (ALKMIM *et al*., 2017; MOSER *et al*., 2018). Thus, the removal of these recalcitrant compounds minimises the fouling potential and cleaning frequency in the desalination steps, reducing the operating costs and increasing the process sustainability (LY *et al*., 2019).

The influence of each individual process in the PRM (photolysis, catalysis, and membrane separation) was investigated (Table 4). To assess the COD removal by the recycled membrane, only filtration (in the darkness and without catalyst dosing) was carried out for 60 min at a pressure of 1.0 bar. The COD retention by the recycled membrane was 9%. The low retention was expected as the wastewater was previously ultrafiltered in the MBR and is consistent with

those reported previously. The COD retention in the recycled membrane suggests that its pore size was smaller than 0.04 μm (UF (MBR) pore size). As reported by Szymański et al. (2018), the contribution of the UF membrane to the PMR is more associated with the catalyst retention than with the removal of pollutants. The COD removal in the photoreactor (44%) was evaluated by operating the PMR bypassing the membrane module. This removal can be associated to photolysis, adsorption, and photocatalysis, which occur simultaneously in the photoreactor. The photolysis contribution to the COD removal (15%) was measured by recirculating the MBR permeate in the PMR under light irradiation and without catalyst dosing and membrane filtration. The COD removal by catalyst adsorption was evaluated by operating the PMR in the darkness bypassing the membrane module. The COD adsorption on the catalyst surface was 8%. According to the mass balance, the photocatalytic contribution was 21%. The multiple comparison Kruskal–Wallis tests confirmed significant differences in removal efficiency between the PMR treatment and photolysis ($p = 0.01582 < 0.05$) as well as between the PMR treatment and membrane process ($p = 0.004306 < 0.05$).

Table 4: Individual contribution of photolysis, catalysis and membrane retention on COD removal in the PMR.

Process	COD removal (%)
PMR	53 ± 4
Photolysis	15 ± 6
Adsorption	8 ± 6
Catalysis	21 ± 6
Membrane	9 ± 3

FTIR spectra of the MBR effluent (PMR feed), PMR permeate, effluent after the photolysis, and recycled membrane permeate are presented in Figure 14 with Y-axis moved for better visualization.

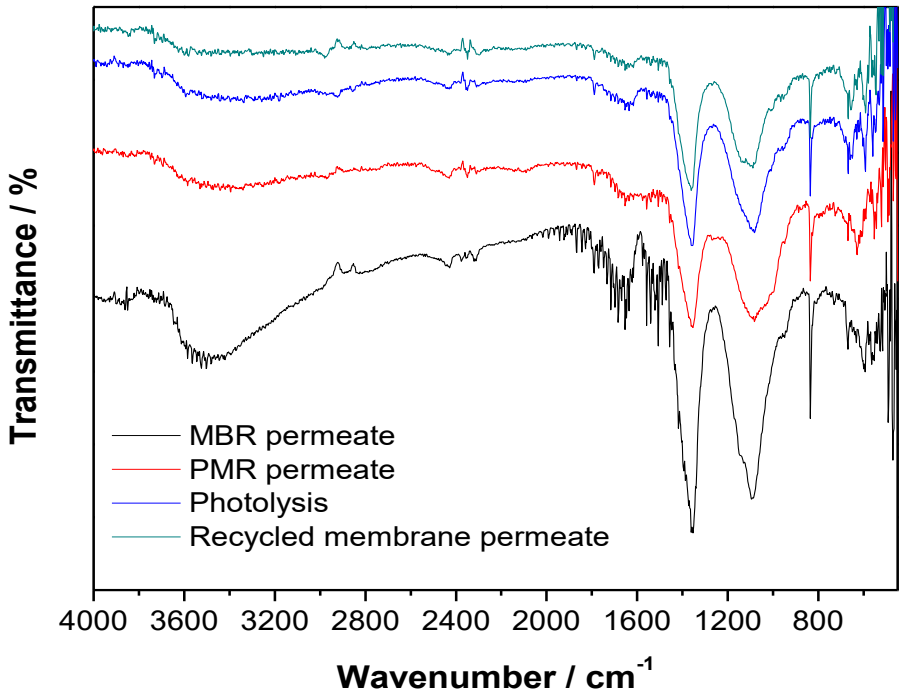

Figure 14: FTIR spectra of the MBR permeate, PMR permeate, effluent after the photolysis, and recycled membrane permeate.

The MBR permeate exhibited several transmittance bands. Most of them are related to EPSs and SMPs produced during the biological process in the wastewater treatment, which may have permeated the membrane (ALKMIM *et al*., 2017). They correspond to the NH stretching of the hydroxyl group in polysaccharides (3300–3500 cm^{-1}), aromatic ring or humic acid (1711 cm^{-1}), amide II (protein secondary structure (possible SMP)) (1620 cm^{-1}), NR symmetrical stretching of -COO- overlapped by amide absorption of amino acids and/or aromatic compounds (1360 cm^{-1}), CC stretching (1076 cm^{-1}), calcium carbonate (864 cm^{-1}), symmetric and asymmetric CO stretchings (1088 cm^{-1}) related to polysaccharide-like substances, and sulphur ($C–SO^{2-}$, S–C) acids in proteins (600 cm^{-1}) (IBRAHIM *et al.*, 2013; PENDASHTEH *et al*., 2011; RAMESH *et al.,* 2006). The bands at 3500, 1711, and 600 cm^{-1} were not observed after the treatment with the whole system, which indicates the removal of the corresponding groups. The other bands exhibited decreased intensities, which reflects their decreased concentrations. In the photolysis and membrane permeation tests, the above bands exhibited reduced intensities, which indicates smaller contributions of these processes to the COD removal in the PMR.

According to the National Institute of Standards and Technology (NIST) infrared database, the raw effluent spectrum is similar to the humic acid spectrum. Significant contents of these compounds in MBR effluents have been reported (JARUSUTTHIRAK and AMY, 2006; MA *et al*., 2014). Besides membrane incrustation, these compounds may lead to the formation of cytotoxic byproducts such as trihalomethanes in later stages of chlorination for disinfection, e.g., in boiler water (MA *et al.*, 2013). This further demonstrates the importance of the process.

When advanced oxidative processes are applied in the wastewater treatment, the evaluation of the toxicities of the generated byproducts is important, as the intermediate compounds formed in the breakdown of the constituent molecules of the effluent can be more dangerous to the living beings and environment than the original compounds (ALFIYA *et al.*, 2017; GOMES JÚNIOR *et al*., 2017). Table 5 shows that the MBR permeate was nontoxic. The effluents treated in the PMR with the green catalyst, photoreactor (only UV light), and membrane system (only membrane) were not toxic (acute toxicity). Although the table 5 shows the toxicity score for the 80 minutes test, at the initial times of 20, 40 and 60 minutes the toxicity was also analyzed and the treated were non-toxic. This is interesting because in the early times of degradation there is a greater propensity to form toxic compounds that are subsequently mineralized with longer residence time (PLAKAS *et al.*, 2016). However, the effluent after the treatment in the PMR with the commercial catalyst was toxic. Therefore, the green catalyst not only had a higher contaminant removal capacity than that of the commercial catalyst, but also did not generate toxic intermediates, whereas the commercial catalyst generated toxic intermediates. This suggests that the two catalysts had different degradation mechanisms and that the green catalyst was more advantageous.

Many studies develop effluents treatments from advanced oxidative processes with the use of UV light and hydrogen peroxide (H_2O_2) and in this route, formations of intermediates more toxic than their parent molecules are reported. In addition, in some cases, all peroxide is not consumed in the reaction generating residual concentration in the treated flow that must be carefully monitored (SPASIANO *et al.*, 2016; MOSER *et al.*, 2018; SZYMAŃSKI *et al.*, 2018). The same was observed in the use of commercial TiO_2 catalyst. Therefore, the process with the use of the green catalyst is a promising alternative considering the percentage of removal of contaminants, small reaction time, absence of chemical consumption, and absence of generation of toxic intermediates.

Table 5: Acute Toxicity (EC 50, 30 min) results for the MBR permeate and treated flows after 80 min of operation in the PMR.

Acute Toxicity (EC 50 – 30 min)				
MBR permeate	**80 min green catalyst – all system**	**80 min commercial catalyst – all system**	**80 min – UV light only**	**80 min – membrane only**
n.t.	n.t.	15.0 ± 1.0	n.t.	n.t.

n.t.: non-toxic; n = 3.

3.3.3 TiO_2 separation efficiency of recycled membrane

To evaluate the TiO_2 retention efficiency of the recycled membrane, the permeates produced in the PMR process were dried in the kiln. The obtained material after the drying was collected and analysed by SEM and EDS (Fig. 15).

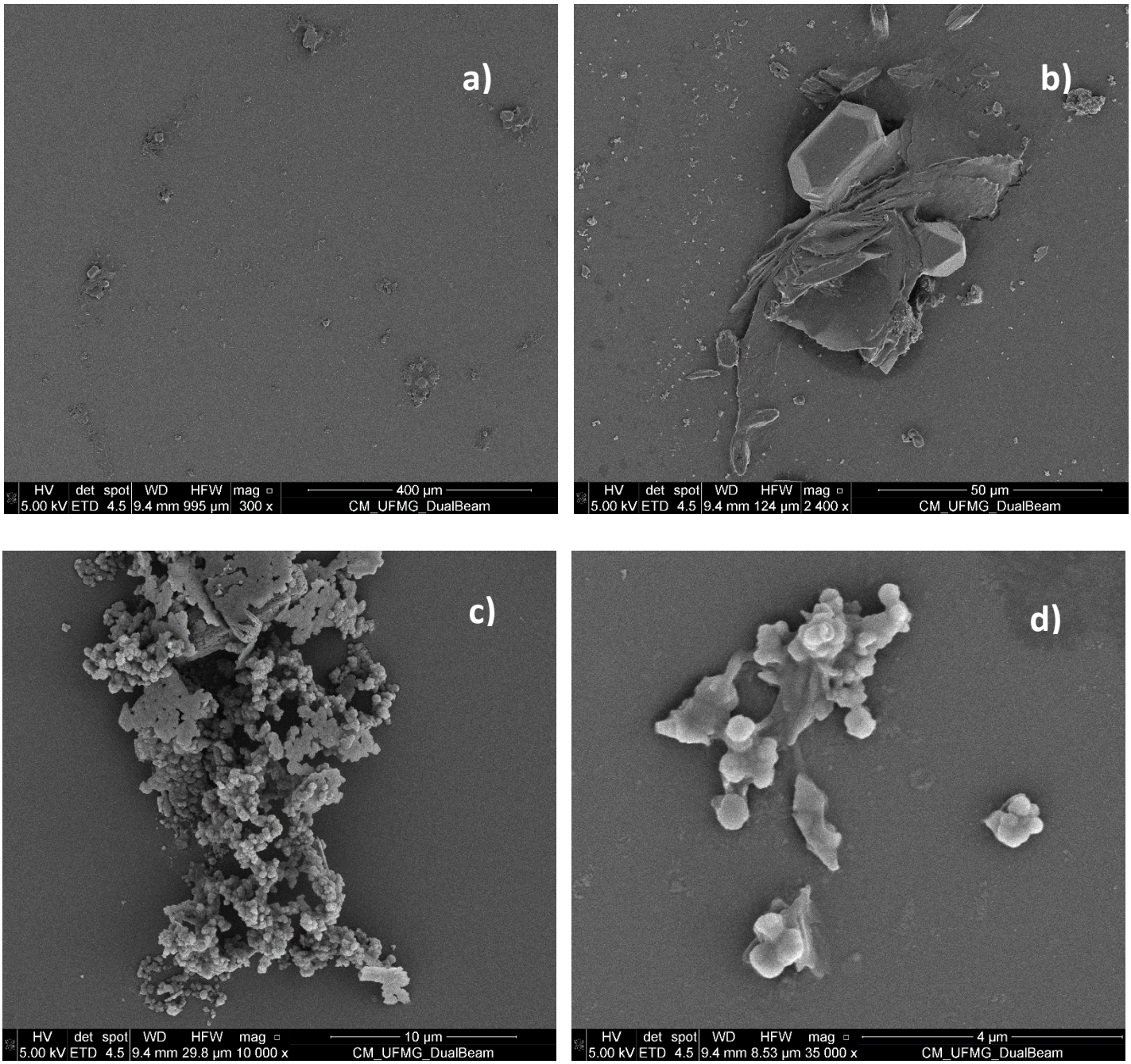

Figure 15: SEM micrographs of different regions of the permeate post drying process at 110°C (a-d); EDS spectrum of the PMR permeate (e).

As shown in the micrographs (Fig. 15 – a-d), the permeate exhibited varying composition with structures of different conformations. The EDS spectra acquired at several points show the presence of organic compounds and salts of sodium, potassium, chlorine, and sulphur. The rather intense absorption peak of silicon originated from the wafer used as the support of the sample. Titanium element was not observed at the analysed points, which confirms its retention in the membrane. This is also demonstrated by the SEM image of the membrane after the permeation with the catalyst deposits (shown in Section 3.3.4).

The high retention of the catalyst by the recycled membrane can be explained by their particle size distributions. The particle size distributions of the green and commercial P25 Degussa catalysts were evaluated (Fig. 16). Both green and commercial catalysts exhibited nanoparticles; in water, they agglomerate on the microscale (LOOSLI *et al.*, 2015). This also facilitates their retention by UF and MF membranes and, consequently, by the recycled membrane with similar characteristics. The green catalyst exhibited a bimodal distribution with average particle sizes of 23 and 743 µm, while the commercial catalyst exhibited a unimodal distribution with a mean size of 49 µm.

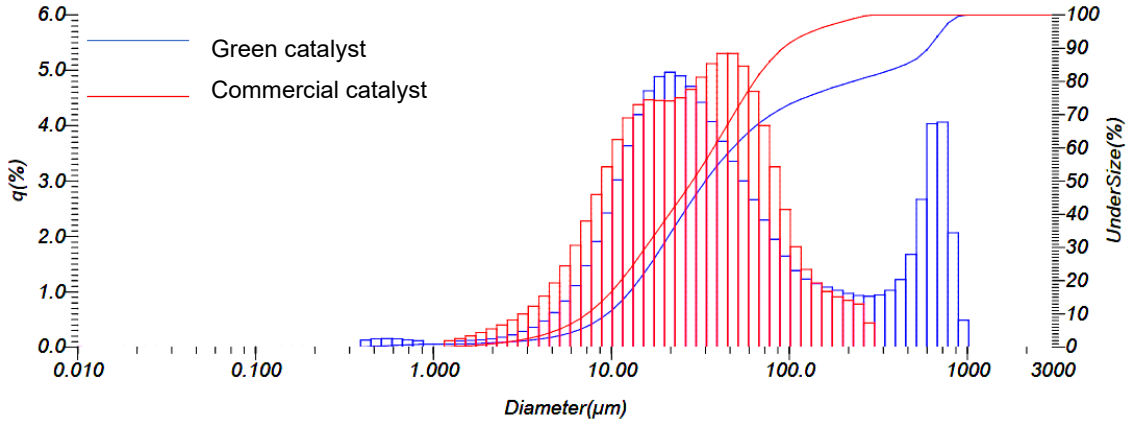

Figure 16: Particle size distribution of the green catalyst and commercial catalyst P25 Degussa.

3.3.4 Membrane performance in the PMR

Figure 17 shows the influences of the green and commercial catalysts on the permeate flux during the oil refinery wastewater treatment by the PMR.

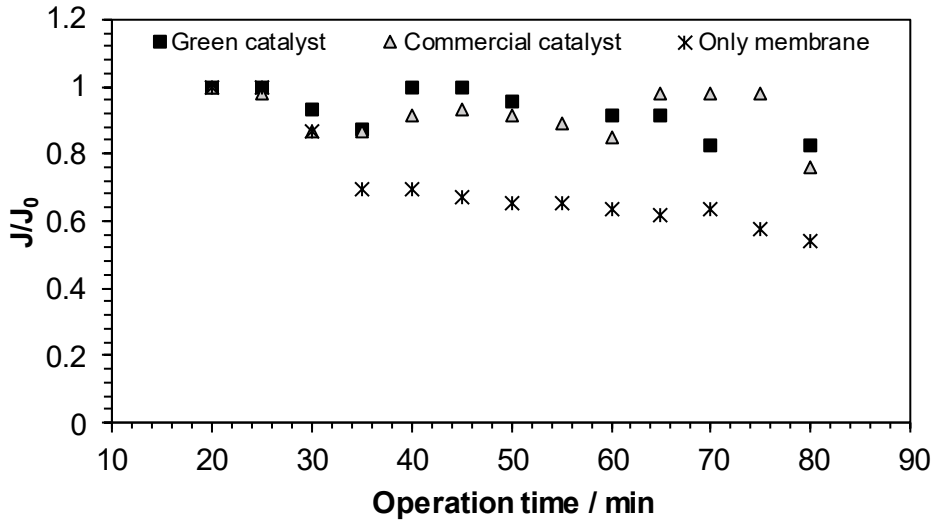

Figure 17: Influences of the green and commercial catalysts on the permeate flux during the treatment of oil refinery wastewater by the PMR (J_0 is the initial flux).

Both synthesised and commercial catalysts contributed to the membrane fouling mitigation, as the FD was lower than 20%. In the absence of catalyst, the FD was larger, 48% at the same monitored time. The results indicate that the catalyst reduced the feed fouling potential owing to the degradation of the compounds in the feed. Similar results were reported by Ho *et al.* (2009), who treated sewage after the biological process in the PMR using commercial TiO_2 and hollow fiber membrane module. The authors observed stability of flow by treating the effluent in the presence of the catalyst in a doubled value in relation to the absence of it.

Note that the green catalyst presented better performance in maintaining the stability of the flow compared to the commercial. However, the differences between the two are small and not statistically significant ($p = 0.891273 > 0.05$). As can be seen in Figure 16, the green catalyst presented a bimodal particle size distribution with particles smaller than the commercial. This difference in size may have contributed to the difference in fouling impacts in some of the monitored times. Smaller particles have fouling potential due to its deposition in the membrane surface, but in the other hand they are more efficient in the degradation of pollutants reducing the fouling occasioned by the feed's organic matter. Similar results with respect to particle size were found by Vela *et al.* (2008) studying the blocking of pores in UF membranes in which smaller particles formed a dense fouling cake, thus creating greater resistance to water flow.

The fouling mitigation by the catalyst was also confirmed by the fouling resistances of the membrane in the PMR system operated with and without the green catalyst, as presented in

Table 6. The fouling resistance of the membrane operated without the catalyst was 7.3 times higher than that operated with the catalyst.

Table 6: Permeate flux in the PMR and hydraulic resistance of the membrane and attributed to the fouling cake.

Flux (L m^2 h^{-1})			Hydraulic resistance (m^{-1})		
J_w	J_{ec}	J_{en}	R_m	R_{fc}	R_{fn}
196.64	161.34	75.63	2.055×10^{12}	4.45×10^{11}	3.29×10^{12}

Jw: permeate water final flux; Jec: final permeate flux with the catalyst; Jen: final permeate flux without the catalyst; Rm: membrane resistance; Rfc: fouling resistance with the catalyst; Rfn: fouling resistance without the catalyst.

SEM images of the recycled membrane after the test in the PMR, chemical elemental map of Ti, and EDS spectrum of the membrane surface are presented in the Figure 18.

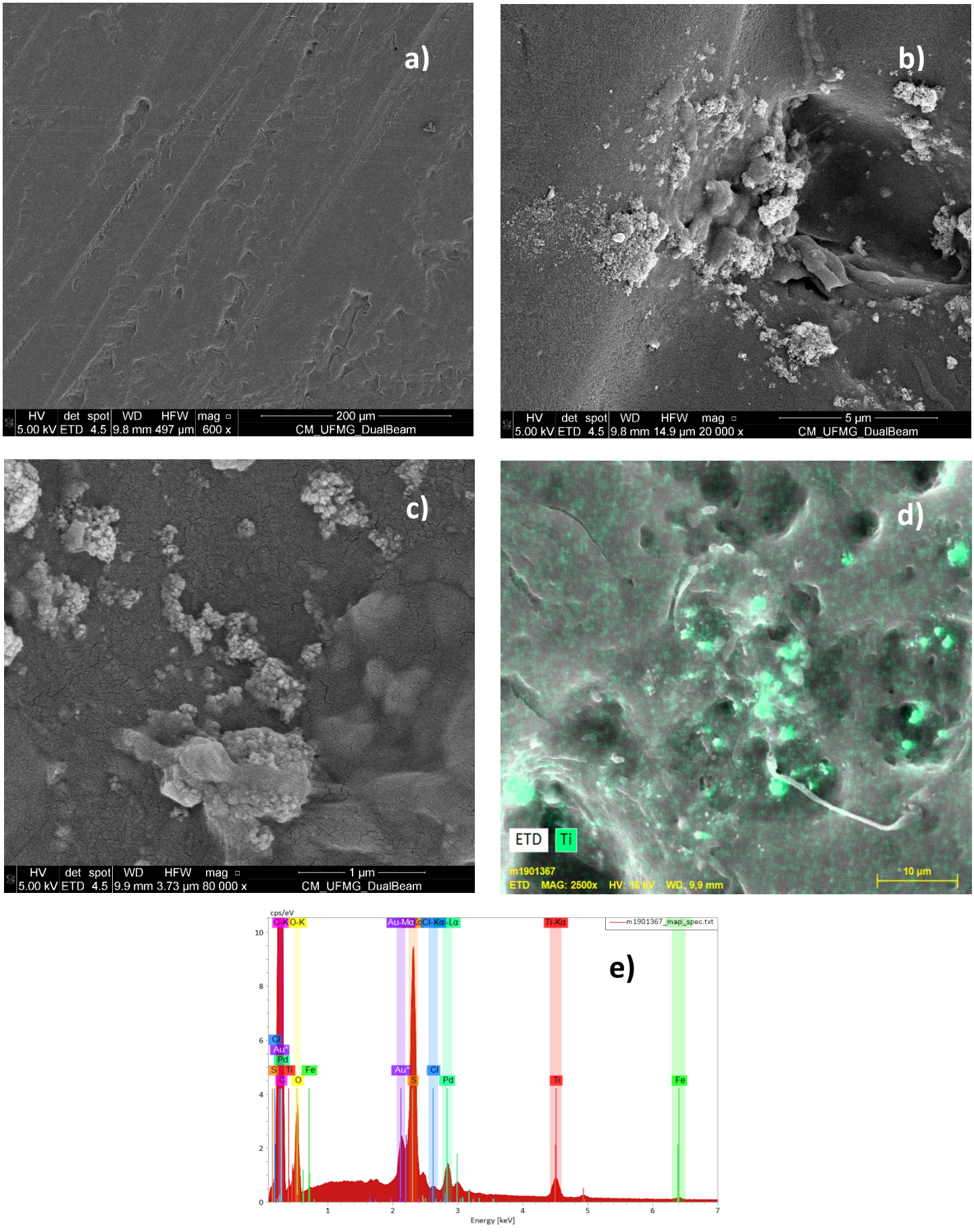

Figure 18: SEM micrographs of different regions and different magnifications of the recycled membrane after the tests in the PMR (a-c), chemical elemental map indicating Ti in the investigated field (d) and EDS spectrum of the membrane surface (e).

The SEM images (Fig. 18-a) do not indicate changes in membrane structure after the PMR operation and successive permeations. Deposits were observed on the membrane surface (Fig. 18-b). The nanoparticles tended to form a cake under the surface of the membrane *(*MOZIA *et al.*, 2015). The oxide (TiO_2) interacted with the membrane, as the deposited particles remained after the physical cleaning with water. Factors such as particle size, membrane pore size, operation pH, and transmembrane pressure may influence the membrane fouling owing to the TiO_2. At a pH of 10, the oxide particle surface was negatively charged as this value is higher than its zero-charge point (pH_{zcp}) of approximately 6.3. At values higher than pH_{zcp}, the particle repulsion is larger, which favours their punctual insertion in the pores, as shown in Figure 18 (b-d) (ZHANG *et al*., 2012).

Although it is possible to verify the fouling formation by TiO_2, it is not very intense, as the formed layer is not thick. The operation of the system at a transmembrane pressure of 1 bar may have contributed to the small thickness of this layer, as a lower operation pressure (0.5–1 bar) in the TiO_2 reactor leads to a lower catalyst deposition, finer fouling layer, and smaller flux reduction (DAROWNA *et al.*, 2017; MOZIA *et al.*, 2015). The chemical elemental map (Fig. 18-d) and EDS spectrum (Fig. 18-e) of the deposits formed on the surface of the membrane indicate the presence of titanium element. The absorption peaks corresponding to gold and palladium elements are related to the employed metallisation, while the small iron peak can be associated to the contamination originating from the system including the pumps, reactor, and connections.

The FTIR spectroscopy data (Fig. 19) suggest that some compounds of the MBR permeate were responsible for the organic membrane fouling. Certain bands in the effluent spectrum, not present in the pristine membrane spectrum, were also observed in the membrane spectrum after the permeation and physical cleaning. They correspond to the NH stretching of hydroxyl groups in polysaccharides (3300–3500 cm^{-1}), CH stretching vibrations of alkenes and alkines (2314 cm^{-1}), aromatic ring or humic acid (1711 cm^{-1}), and NR symmetrical stretching of -COO- overlapped by amide absorption of amino acids and/or aromatic compounds (1360 cm^{-1}) (LINGBO *et al.,* 2005, IBRAHIM *et al*., 2013, MARTINI *et al.,* 2017). These observations are consistent with previous studies where protein-like structures and carbohydrates were characterised as fouling-causing agents in MBR systems (CHEN *et al.,* 2017; TIAN *et al*., 2012). The results corroborate the previously discussed data regarding SMPs and EPSs.

Although such compounds were identified on the surface of the membrane, their impact on the decrease in flux was substantially reduced by the catalyst presence, as shown in Figure 17.

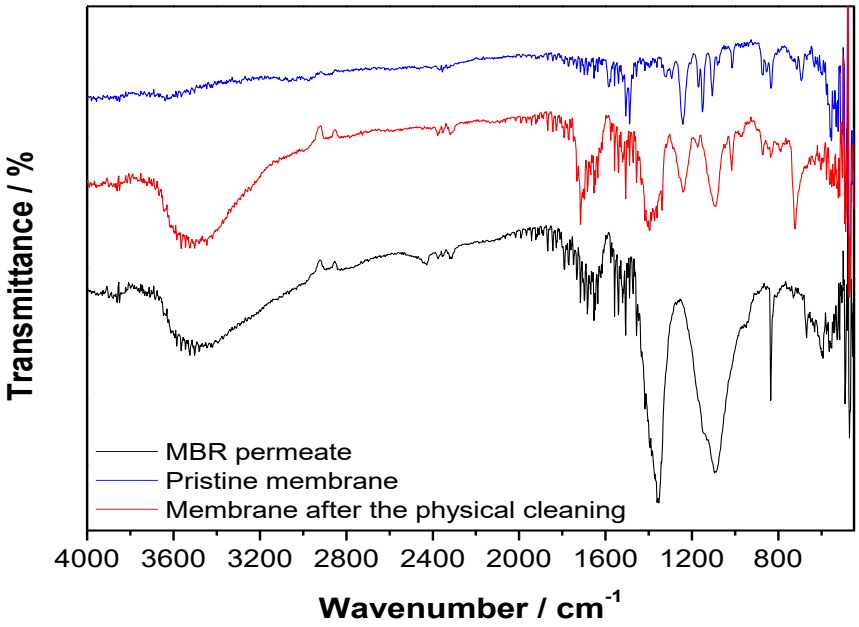

Figure 19: FTIR spectra of the MBR permeate, pristine membrane, and membrane after the physical cleaning.

3.3.5 Photocatalytic and membrane stability

To evaluate the stability of the membrane upon the successive tests and effectiveness of the catalyst after several operations, reuse tests were carried out with the same green catalyst, complementing only the volume of the feed. Figure 20 shows the permeate flux behaviour of the membrane over time, after the successive catalyst reuses.

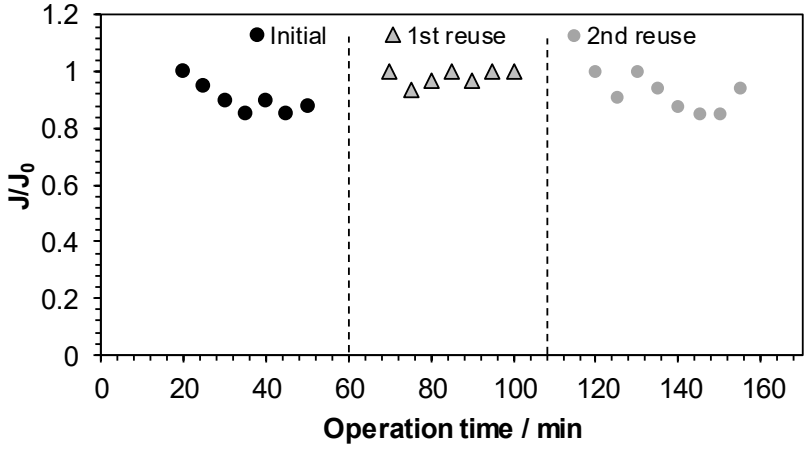

Figure 20: Permeate flux over time in the catalyst reuses in the PMR.

From Figure 20, it is noted that the fluxes locate in a narrow oscillation range, with a maximum decrease of 15% compared to its initial value, indicating that the membrane does not degrade during the process. The same median range is maintained throughout the experiments ($p = 0.11456 > 0.05$). As can be seen in the operation time equal to 70 minutes, the flow returns to its initial value at the first reuse, showing the reversibility of the fouling caused by the catalyst. An increase in flux beyond the initial one is characteristic of the degradation of the membrane due to the abrasion caused by the catalyst (MOZIA *et al.*, 2015; DAROWNA *et al.*, 2017), which was not observed in the process.

Reduction of the flow due to the catalyst, although it exists, is small, because the porous structure of the catalyst has low resistance to water flow (LEE *et al.*, 2002). It is important to mention that the tests were conducted with the pH of the effluent corrected to 10, according to the best performances of the catalyst previously studied and, generally, in alkaline pHs, the photocatalytic degradation is increased and there is a lower deposition of the particles in the membrane (DAMODAR *et al.*, 2012; ZHANG *et al.*, 2016). This is because the agglomeration between the particles is influenced by the pH of the medium and at pHs higher than their zeta potential ($pH_{zpc} = 6.3$) the TiO_2 has its surface negatively charged, promoting a high repulsion of the particles which favors a high rejection of the particles as well as lower encrustation (JANSSENS *et al.*, 2017; MOLINARI *et al.*, 2017).

Figure 21 presents the TGA results of the recycled membrane before and after permeation.

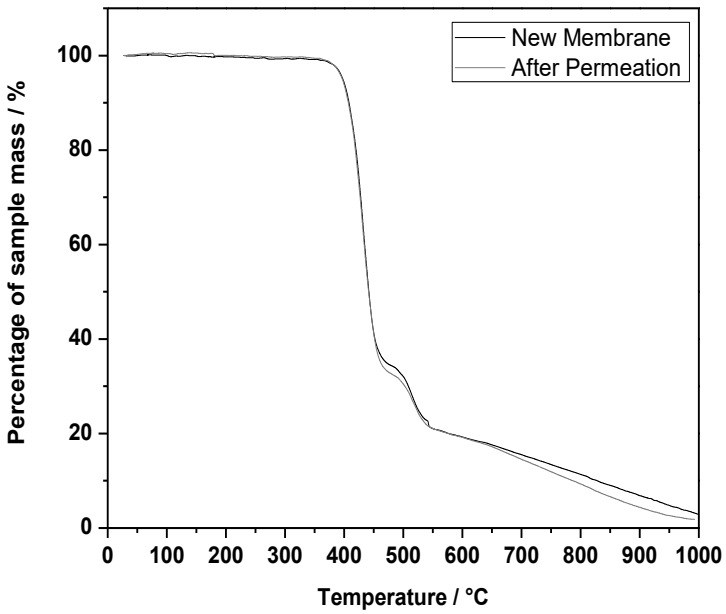

Figure 21: Thermal decomposition curves of the recycled membrane before and after permeation at a heating program of 10 °C min^{-1} in the range of 33 to 1000 °C.

The TGA (Fig. 21) confirmed the absence of degradation of the membrane by the catalyst, as the losses of membrane mass as a function of the temperature before and after the experiments were very similar and, thus, endorse the maintaining of the flow as previously described.

The membrane decomposition temperatures before and after the permeation were approximately 380 °C, which is consistent with the literature data for polyethersulfone membranes in the range of 350 to 480 °C (LI *et al*., 2009; RAZMJOU *et al*., 2011). For the new membrane, the highest percentage of mass reduction was approximately 65%, while the residual mass percentage was 3.6%, while those of the membrane after permeation were 67% (at the same temperature) and 3.6%, respectively. As aforementioned, for the reason that the membranes have undergone an oxidative recycling process, different thicknesses of the selective layer may have been removed in different regions of the membrane and this factor is attributed to this small difference of the percentages found and not to the degradation in reason of the catalyst.

Finally, Figure 22 show normalized COD, ABS_{254} removal and TN removal in the catalyst reuses in the PMR.

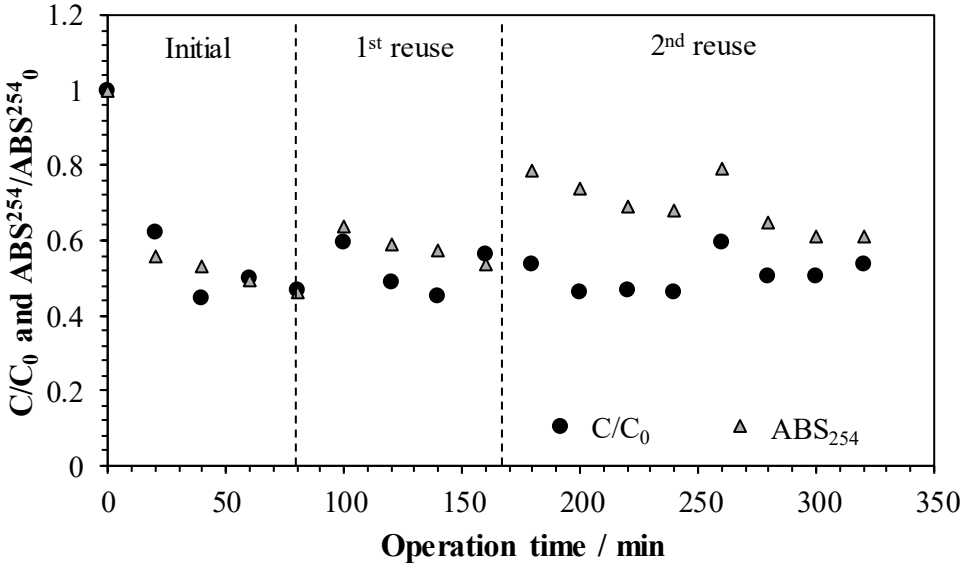

Figure 22: Normalised COD and ABS_{254} reductions during the catalyst reuses in the PMR.

As observed in the fluxes in Figure 20, photocatalysis also maintains its stability throughout the experiments (Fig. 22). It can be seen that with the advancement of the operating time, there is an increase in the percentage of removal of contaminants in terms of COD, which is associated to the longer residence time of the contaminants in contact with the irradiated catalyst. Thus, at 80 minutes in the initial test a COD removal of 54% was achieved. It is worth noting that, as can be seen in the first reuse, the catalyst regenerates its initial capacity, showing that the adsorbed compounds on its surface are degraded and the active sites are again available for reaction. A percentage of 55% removal was achieved at the first time reuse of 140 minutes which equals 60 minutes passed from the start of the first reuse. Analogously, 56% removal is obtained within 60 minutes of the second reuse test. It can be concluded, therefore, that the photocatalysis process is stable in the studied system. A major part of the previous studies involving the use of TiO_2 catalyst in PMRs used concentrations varying from 0.5 g L^{-1} to 2.5 g L^{-1} (IGLESIAS *et al.*, 2016; DAROWNA *et al.*, 2017) achieving organic matter removal around 50% in 120 minutes operation. The catalyst concentration used at this work (0.1 g L^{-1}) reached the same percentages in lower times, as 40 minutes, for example.

Throughout the reuses, the system reduced ABS_{254}, but a certain decrease in capacity was observed, owing to the accumulation of refractory compounds during the experiment. When the reuse cycle was initiated, an MBR permeate was added to the residual volume to obtain the initial feed volume. This decrease in capacity may be also associated with a possible loss of catalyst particles in the system (deposition on the membrane surface, deposition on the reactor

walls and piping), as described by (PLAKAS *et al.*, 2016). Therefore, we developed a stable photocatalyst and effective PMR system for the removal of recalcitrant organic compounds.

3.4 CONCLUSIONS

PMR with TiO_2 and recycled membrane proved to be a promising technology for tertiary treatment of oil refinery wastewater, since it was able to promote removals of recalcitrant organic matter remaining from MBR expressed as COD up to approximately 60%. The reusability of the catalyst was confirmed based on the maintenance of degradation percentages of the initial tests and it was verified that the catalyst has the greatest impact on the removal of COD with contribution of the membrane and the incidence of UV-C light in minor scale. The decay of the absorbance values at 254 nm was found around 54% and indicates that aromatic compounds as phenols are removed by the process. Green TiO_2 catalyst showed a better performance than the commercial one in the terms of pollutants removal. The permeate flux decline was lower than 20% in the catalyst presence and 46% in its absence. As well as membrane resistance values due to fouling were 7.3 times higher in the system operated in the absence of the catalyst. The recycled membrane was able to retain the catalyst as confirmed by SEM, TGA and EDS. No degradation of the membrane was observed by the catalyst use. The MBR permeate is constituted mainly of SMP and EPS substances that had their concentration reduced by the PMR as shown by FTIR and COD removals.

In view of the above stated, PMR with green catalyst and recycled RO membrane has proved to be an efficient process for oil refinery tertiary treatment, with beneficial effects to the membrane and to the catalyst, achieving high recalcitrant pollutants removal percentages and generating high quality effluent suitable for reuse. Another possibility is to constitute a previous step which generates a better feature flow for the polishing processes with reverse osmosis membranes reducing the fouling.

CHAPTER 4

Final considerations

The present work aimed the development of a photocatalytic membrane reactor that conciliates environmental friendly units by the association of TiO_2 catalyst produced by a cleaner route of synthesis with time and reagents savings and the recycled reverse osmosis membrane. The system was evaluated for the treatment of refinery effluent.

Synthesis showed to be efficient for the formation of pure titanium dioxide nanoparticles in the anatase phase with a mean crystallite size of 14 nm. It is interesting to note the oxide formation in a single phase presented effectiveness in the degradation of organic molecules, according to standard test carried out with methylene blue, in which 95% degradation was achieved in 300 minutes of reaction in the presence of UV-C light. In addition, a high adsorptive capacity of the particles was verified.

In small reaction times and low concentrations, the synthesized catalyst proved to be effective in removing recalcitrant compounds from the refinery effluent. At 90 minutes of reaction, 32% and 67% of TOC and TN removal were achieved, respectively, in the best condition tested of 100 mg L^{-1} catalyst concentration and pH 10. From these results it was noted that specifically this effluent after treatment process in the MBR has characteristics that favor its treatment in basic conditions, which implies consumption of chemicals for pH adjustment. It is emphasized that each effluent according to its characteristics will have different better operating conditions of the catalyst performance.

Among the catalyst concentrations studied, the lowest showed better performance in the removal of TOC. The Electrical Energy per Order (EE_0) in this condition was 356.29 KWh m^{-3} $order^{-1}$ the minor among the calculated. The catalyst was shown to be stable for reuse at least four times what associated to the best catalyst concentration calculated and the EE_0 value is interesting from an economic point of view and for stagger the process. The fact that the catalyst can be used in successive batches makes it competitive among other advanced oxidative processes that use chemicals that are consumed in the reaction and consequently generate an impact on operating costs.

The use of the catalyst has proved to be promising for the treatment of the refinery effluent and the results are even more interesting when considering that the constituents of this treated stream are recalcitrant from previous biological treatment. It may, therefore, consist of a step prior to polishing processes for reuse, such as reverse osmosis, reducing fouling in the membranes caused by the effluent compounds. In order to obtain higher rates of contaminants

removal, modifications in the structure of the catalyst or use of chemicals should be studied. Another point to be evaluated is how to retain such nanoparticles in the reaction medium for reuse. Hence the motivation of hybrid PMR development.

The coupling of the catalyst to the recycled membrane showed beneficial results for both operations. Firstly, because the membrane was efficient in the retention of the catalyst and its confinement in the system. In addition, higher flow stabilities were noted when the system operated in the membrane separation associated with photocatalysis.

The PMR was able to promote removals of organic matter remaining from MBR expressed as COD up to approximately 60%. As the catalyst, the incidence of UV light alone and permeation through the membrane were able to remove some contaminants, but on a smaller scale, showing that the greatest function of the membrane in the system was the retention of the catalyst. It was noted by the advancement of the removals over time that the membrane contributed to a longer residence time of the undegraded compounds inside the reactor. In addition, values above 50% absorbance removal at 254 nm were found, which is an interesting result from the point of view of removal of complex double- and triple-bonded pollutants such as phenols.

While in 80 minutes of operation of the recycled membrane in the treatment of the used effluent a decrease of 46% of the flux was registered, with the presence of the catalyst the decrease was of 18%, which concludes that the catalyst has a positive impact on maintaining the membrane permeate flux. Consequently, it can generate lower backwash frequencies, lower operational stops, lower membrane turnover and lower costs. Microscopies of the membranes before the treatment batches showed a layer with certain discontinuities reflecting that the oxidative process generated pores in the membrane leaving it in terms of selectivity intermediated between a UF and MF membrane. However, in spite of the pores, the membrane proved to be effective in catalyst retention since catalyst deposits were observed on the membrane surface after the tests, as well as EDS analysis of the permeates did not detect the titanium element in any of the fields surveyed. Moreover, in suspension the catalyst is in the form of agglomerates of micrometric order (23 μm and 743 μm - synthesized) and 49 μm (commercial), which facilitates retention by the membrane.

The FTIR analyzes showed functional groups characteristic of microbial products as SMP e EPS in the effluent and that some of them were removed in the treatment by the disappearance of 3300 cm^{-1}, 1620 cm^{-1} and 609 cm^{-1} bands. This result endorses the benefits of treatment for

further polishing steps such as reverse osmosis and nanofiltration by mitigating fouling, or facilitating concentrate treatment processes such as crystallization, as well as reducing the risk of formation of toxic compounds in disinfection processes that use chlorination.

It is noteworthy that the performance of the catalyst synthesized in terms of organic matter removal as well as permeate flux stability of the membrane was superior to that of the commercial one. In addition, none of the treated flows with the synthesized catalyst generated currents with toxicity, which reinforces its potential in the safe treatment of effluents. Differently from the commercial one that in 80 minutes of reaction evaluated produced toxic intermediates.

With the results obtained, it was verified that the coupling of the catalyst to the membrane caused synergistic effects to both technologies and that this could be a promising alternative in the treatment of refinery effluents with a view to the generation of water of such quality that it reduces operational costs in steps of polishing or even propitious to direct reuse in less noble ends.

CHAPTER 5

Suggestions for future works

Suggestions for future work include:

- Evaluation of the performance of other membranes as nanofiltration in the PMR at the parameters: removal of the recalcitrant compounds, ions removal, fouling reduction and flux stabilization;

- The evaluation of the impact of the parameters luminous intensity and feed concentration on the pollutants removal in the PMR;

- The evaluation of the effectiveness of the system dealing with raw oil refinery effluent regarding removal of organic matter;

- Economic analysis of the treatment in the PMR process;

- PMR's efficiency comparison treating oil refinery effluent in two different configurations: TiO_2 catalyst suspended in the medium and immobilized on the membrane surface.

CHAPTER 6

References

ABASS, O.K.; FANG, F.; ZHUO, M.; ZHANG, K. Integrated interrogation of causes of membrane fouling in a pilot-scale anoxic-oxic membrane bioreactor treating oil refinery wastewater. *Science of the Total Environment*, v. 642, p. 77-89, 2018.

ABDEL-MAKSOUD, Y.K.; IMAM, E.; RAMADAN, A.R. TiO_2 water-bell photoreactor for wastewater treatment. *Solar Energy*, v. 170, p. 323-335, 2018.

ABDELWAHAB, O.; AMIN, N.K.; EL-ASHTOUKHY, E-S.Z. Electrochemical removal of phenol from oil refinery wastewater. *Journal of Hazardous Materials*, v. 163, n. 2-3, p. 711-716, 2009.

AHMED, S.N.; HAIDER, W. Heterogeneous photocatalysis and its potential applications in water and wastewater treatment: a review. *Nanotechnology*, v. 29, n. 34, p. 342001-3420032, 2018.

AKITA, T.; KOHYAMA, M. Visualization of the distribution of anatase and rutile TiO_2 crystals in Au/TiO_2 powder catalysts by STEM-EELS spectrum imaging. *Surface and Interface Analysis*, v. 46, n. 12-13, p. 1249-1252, 2014.

AKPAN, U.G.; HAMEED, B.H. Development and photocatalytic activities of TiO_2 doped with CaeCeeW in the degradation of acid red 1 under visible light irradiation, *Desalination and Water Treatment*, v. 52, p. 5639-5651, 2013.

AKPAN, U.G.; HAMEED, B.H. Parameters affecting the photocatalytic degradation of dyes using TiO_2-based photocatalysts: a review. *Journal of Hazardous Materials*, v. 170, p. 520-529, 2009.

ALFIYA, Y.; ERAN, F.; JANIN, W.; OLIVER, O.; YAEL, D. Photodegradation of micropollutants using V-UV/UV-C processes; Triclosan as a model compound. *Science of the Total Environment*, v. 601–602, p. 397–404, 2017.

ALJUBOURY, D.A.D.A.; PALANIANDY, P.; AZIZ, H.B.A.; FEROZ, S. Comparison and performance of petroleum wastewater treatment using photocatalytic TiO_2, photo Fenton, TiO_2/Fenton and TiO_2/Fenton/ZnO processes. *Water Resources and Industry*, p. 16-39, 2016.

ALJUBOURY, D.D.A.; PALANIANDY, P.; ABDUL, A.H.B.; FEROZ, S. Treatment of petroleum wastewater by conventional and new technologies-A review. *Global Nest Journal*, v. 19, p. 439-452, 2017.

ALKMIM, A.R.; COSTA, P.R.; MOSER, P. B.; NETA, L.S.F.; SANTIAGO, V.M.J.; CERQUEIRA, A.C.; REIS, B.G.; AMARAL, M.C.S. Potential use of membrane bioreactor to treat petroleum refinery effluent: comprehension of dynamic of organic matter removal, fouling

characteristics and membrane lifetime. *Bioprocess and Biosystems Engineering*, v. 40, n. 12, p. 1839-1850, 2017.

ALKMIM, A.R.; COSTA, P.R.; MOSER, P.B.; NETA, L.S.F.; SANTIAGO, V.M.J.; CERQUEIRA, A.C.; AMARAL, M.C.S. Long-term evaluation of different strategies of cationic polyelectrolyte dosage to control fouling in a membrane bioreactor treating refinery effluent. *Environmental Technology*, v. 37, n. 8, p. 1026-1035, 2015.

ALSALHY, Q.F.; ALMUKHTAR, R.S.; ALANI, H.A. Oil refinery wastewater treatment by using Membrane Bioreactor (MBR). *Arabian Journal for Science and Engineering*, v. 41, n. 7, p. 2439-2452, 2015.

ALTURKI, A.; ALTURKI, A.; MCDONALD, J.; KHAN, S.J.; HAI, F.I.; PRICE, W.E.; NGHIEM, L.D. Performance of a novel osmotic membrane bioreactor (OMBR) system: Flux stability and removal of trace organics. *Bioresource Technology*, v. 113, p. 201–206, 2012.

ALVA-ARGÁEZ, A.; KOKOSSIS, A. C.; SMITH, R. The design of water-using systems in petroleum refining using a water-pinch decomposition. *Chemical Engineering Journal*, v. 128, n. 1, p. 33–46, 2007.

AMARAL, M.C.S.; NETA, L.S.F.; BORGES, C.P.; CERQUEIRA, A.C.; TORRES, A.P.; FLORIDO, P.L.; SANTIAGO, V.M.J. Treatment of refinery effluents by pilot membrane bioreactors: pollutants removal and fouling mechanism investigation. *Desalination and Water Treatment*, v. 56, n. 3, p. 583-597, 2014.

ANI, I.J.; AKPAN, U.G.; OLUTOYE, M.A.; HAMEED, B.H. Photocatalytic degradation of pollutants in petroleum refinery wastewater by TiO_2- and ZnO-based photocatalysts: Recent development. *Journal of Cleaner Production*, v. 205, n.1, p. 930-954, 2018.

APHA. *Standard methods for the examination of water and waste water*. American Public Health Association, Washington, DC, 21st edn. 2005.

AZEEZ, F.; AL-HETLANI, E.; ARAFA, M.; ABDELMONEM, Y.; NAZEER, A.A.; AMIN, M.O.; MADKOUR, M. The effect of surface charge on photocatalytic degradation of methylene blue dye using chargeable titania nanoparticles. *Scientific Reports,* v. 8, n. 1, p. 1-9, 2018.

BAYAT, M.; MEHRNIA, M. R.; HOSSEINZADEH, M.; SHEIKH-SOFLA, R. Petrochemical wastewater treatment and reuse by MBR: A pilot study for ethylene oxide/ethylene glycol and olefin units. *Journal of Industrial and Engineering Chemistry*, v. 25, p. 265-271, 2015.

BEHNAJADY, M.A.; VAHID, B.; MODIRSHAHLA, N.; SHOKRI, M. Evaluation of electrical energy per order (EEO) with kinetic modeling on the removal of Malachite Green by US/UV/H_2O_2 process. *Desalination*, v. 249, n. 1, p. 99-103, 2009.

BENITO-ALCÁZAR, C.; VINCENT-VELA, M. C.; GOZÁLVEZ-ZAFRILLA, J. M.; LORA-GARCÍA, J. Study of different pretreatments for reverse osmosis reclamation of a petrochemical secondary effluent. *Journal Of Hazardous Materials*, v. 178, n. 1-3, p. 883-889, 2010.

BESSEKHOUAD Y.; ROBERT, D.; WEBER, J.V. Synthesis of photocatalytic TiO_2 nanoparticles: optimization of the preparation conditions, *Journal of Photochemistry and Photobiology A. Chemistry*., v. 157, p. 47–53, 2003.

BHATTACHARYA, M.; BASAK, T. A review on the susceptor assisted microwave processing of materials. *Energy 97*, p. 306–338, 2016.

BREGADIOLLI, B.A.; FERNANDES, S. L.; GRAEFF, C.F.O. Easy and fast preparation of TiO_2 - based nanostructures using microwave assisted hydrothermal synthesis. *Materials Research,* v. 20, n. 4, p. 912-919, 2017.

CABELLO, G.; DAVOGLIO, R.A.; PEREIRA, E.C. Microwave-assisted synthesis of anatase-TiO_2 nanoparticles with catalytic activity in oxygen reduction. *Journal of Electroanalytical Chemistry*, v. 794, p. 36-42, 2017.

CAPODAGLIO, A.G.; HLAVINEK, P. Physico-chemical technologies for nitrogen removal from wastewaters: a review. *Ambiente e Agua - An Interdisciplinary Journal of Applied Science*, p. 481-498, 2015.

CHAUHAN, R.; KUMAR, A.; CHAUDHARY, R. Structural and optical characterization of Ag-doped TiO_2 nanoparticles prepared by a sol–gel method. *Research on Chemical Intermediates*, v. 38, n. 7, p. 1443-1453, 2012.

CHEN, D.; HUANG, F.; CHENG, Y.B.; CARUSO, R.A. Mesoporous anatase TiO_2 beads with high surface areas and controllable pore sizes: a superior candidate for high-performance dye-sensitized solar cells. *Advanced Materials*, v. 21, n. 21, p. 2206-2210, 2009.

CHEN, M.; ZHANG, X.; WANG, Z.; WANG, L.; WU, Z. QAC modified PVDF membranes: antibiofouling performance, mechanisms, and effects on microbial communities in an MBR treating municipal wastewater. *Water research*, v. 120, p. 256-264, 2017.

CHEN, Q.; YU, Z.; LI, F.;YANG, Y.; PAN, Y.; PENG, Y.; YANG, X.; ZENG, G. A novel photocatalytic membrane decorated with RGO-Ag-TiO_2 for dye degradation and oil–water emulsion separation. *Journal of Chemical Technology and Biotechnology*, v. 93, n. 3, p. 761–775, 2018.

CHIOU, C-H.; WU, C-Y.; JUANG, R-S. Photocatalytic degradation of phenol and m-nitrophenol using irradiated TiO2 in aqueous solutions. *Separation and Purification Technology*, v. 62, n. 3, p. 559-564, 2008.

CHOU, J-C.; LIAO, L.P. Study on pH at the point of zero charge of TiO_2 pH ion-sensitive field effect transistor made by the sputtering method. *Thin Solid Films*, v. 476, n. 1, p. 157-161, 2005.

CORRADI, A.B.; BONDIOLI, F.; FOCHER, B.; FERRARI, A.M.; GRIPPO, C.; MARIANI, E.; VILLA, C. Conventional and Microwave-Hydrothermal Synthesis of TiO_2 Nanopowders. *Journal of the American Ceramic Society*, v. 88, n. 9, p. 2639-2641, 2005.

COSENZA, A; DI BELLA, G.; MANNINA, G.; TORREGROSSA, M. The role of EPS in fouling and foaming phenomena for a membrane bioreactor. *Bioresearch Technology*, v. 147, p. 184-192, 2013.

COUTINHO DE PAULA, E.; SANTOS AMARAL, M. C. Environmental and economic evaluation of end-of-life reverse osmosis membranes recycling by means of chemical conversion. *Journal of Cleaner Production*, v. 194, p. 85–93, 2018.

COWARD, T.; TRIBE, H.; HARVEY, A.P. Opportunities for process intensification in the UK water industry: A review. *Journal of Water Process Engineering*, v. 21, p.116-126, 2018.

DAMODAR, R. A.; YOU, S. J.; CHIOU, G. W. Investigation on the conditions mitigating membrane fouling caused by TiO_2 deposition in a membrane photocatalytic reactor (MPR) used for dye wastewater treatment. *Journal of Hazardous Materials*, v.203-204, p.348-356, 2012.

DAROWNA, D.; Wróbel, R.; MORAWSKI, A.W.; MOZIA, S. The influence of feed composition on fouling and stability of a polyethersulfone ultrafiltration membrane in a photocatalytic membrane reactor. *Chemical Engineering Journal*, v. 310, p. 360–367, 2017.

DE PAULA, E. C.; GOMES, J. C. L.; AMARAL, M. C. S. Recycling of end-of-life reverse osmosis membranes by oxidative treatment: A technical evaluation. *Water Science and Technology*, v. 76, n. 3, p. 605–622, jul. 2017.

DIYA'UDDEEN, B. H.; DAUD, W.M.A.W.; AZIZ, A.R.A. Treatment technologies for petroleum refinery effluents: a review. *Process Safety and Environmental Protection*, v. 89, n. 2, p. 95-105, 2011.

DOMINGOS, R.A.; FONSECA, F.V. Evaluation of adsorbent and ion exchange resins for removal of organic matter from petroleum refinery wastewaters aiming to increase water reuse. *Journal of Environmental Management*, v. 214, p. 362-369, 2018.

DONOSE, B. C.; SUKUMAR, S.; PIDOU, M.; POUSSADE, Y.; KELLER, J.; GERNJAK, W. Effect of pH on the ageing of reverse osmosis membranes upon exposure to hypochlorite. *Desalination*, v. 309, p. 97–105, 2013.

DOW. Reverse Osmosis Membranes Technical Manual. DOW FILMTEC™, 2012. Disponível em:<http://msdssearch.dow.com/PublishedLiteratureDOWCOM/dh_095b/0901b8038095b91d.pdf?filepath=liquidseps/pdfs/noreg/609-00071.pdf>. Acesso em: 08 de maio de 2019.

DRIOLI, E.; STANKIEWICZ, A.I.; MACEDONIO, F. Membrane engineering in process intensification — an overview. *Journal of Membrane Science,* v. 380, n. (1-2), p. 1-8., 2011.

DU, J. R.; PELDSZUS, S.; HUCK, P.M.; FENG, X. Modification of membrane surfaces via microswelling for fouling control in drinking water treatment. *Journal of Membrane Science*, v. 475, p. 488–495, 2015.

ELSELLAMI, L.; DAPPOZZE, F.; FESSI, N. Highly photocatalytic activity of nanocrystalline TiO_2 (anatase, rutile) powders prepared from $TiCl_4$ by sol–gel method in aqueous solutions. *Process Safety and Environmental Protection*, v. 113, p. 109–121, 2017.

ESTRADA-ARRIAGA, E.B.; ZEPEDA-AVILES, J.A.; GARCÍA-SÁNCHEZ, L. Post-treatment of real oil refinery effluent with high concentrations of phenols using photo-ferrioxalate and Fenton's reactions with membrane process step. *Chemical Engineering Journal*, v. 285, p. 508-516, 2016.

FALK, G. S.; BORLAF, M.; LÓPEZ-MUÑOZ, M. J.; FARIÑAS, J. C.; NETO, J. R.; MORENO, R. Microwave-assisted synthesis of TiO_2 nanoparticles: photocatalytic activity of powders and thin films. *Journal Of Nanoparticle Research*, v. 20, n. 2, p. 1-10, 2018.

FARAJNEZHAD, H.; GHARBANI, P. Coagulation treatment of wastewater in petroleum industry using poly aluminum chloride and ferric chloride. *International Journal Research Review Applied Science,* v. 13, p. 306-310, 2012.

FIGUEROLA, E.L.M.; ERIJMAN, L. Diversity of nitrifying bacteria in a full-scale petroleum refinery wastewater treatment plant experiencing unstable nitrification. *Journal of Hazardous Materials*, v. 181, n. 1-3, p. 281-288, 2010.

FILIPPO, E.; CAPODILUPO, A.L.; CARLUCCI, C.; PERULLI, P.; CONCIAURO, F.; CORRENTE, G.A.; CICCARELLA, G. Efficient, Green Non-Aqueous Microwave-Assisted Synthesis of Anatase TiO_2 and Pt Loaded TiO_2 Nanorods with High Photocatalytic Performance. *Nanomaterials and Nanotechnology*, v. 5, p. 31-38, 2015.

FRUNZA, L.; DIAMANDESCU, L.; ZGURA, I.; FRUNZA, S.; GANEA, C.P.; NEGRILA, C.C.; ENCULESCU, M.; BIRZU, M. Photocatalytic activity of wool fabrics deposited at low temperature with ZnO or TiO_2 nanoparticles: methylene blue degradation as a test reaction. *Catalysis Today*, v. 306, p. 251-259, 2018.

FU, J.; JI, M.; WANG, Z.; JIN, L.; AN, D. A new submerged membrane photocatalysis reactor (SMPR) for fulvic acid removal using a nano-structured photocatalyst. *Journal of Hazardous Materials*, v. 131, n. 1–3, p. 238–242, 2006.

GARCÍA-PACHECO, R.; LANDABURU-AGUIRRE, J.; MOLINA, S.; RODRÍGUEZSÁEZ, L.; TELI, S.B.; GARCÍA-CALVO, E. Transformation of end-of-life RO membranes into NF and UF membranes: Evaluation of membrane performance. *Journal of Membrane Science*, v. 495, p. 305-315, 2015.

GARCÍA-PACHECO, R.; LANDABURU-AGUIRRE, J.; TERRERO-RODRÍGUEZ, P.; CAMPOS, E.; MOLINA-SERRANO, F., RABADÁN, J.; GARCÍA-CALVO, E. Validation of recycled membranes for treating brackish water at pilot scale. *Desalination*, v. 433, p. 199–208, 2018.

GOMES JÚNIOR, O.; NETO, W. B.; MACHADO, A. E.; DANIEL, D.; TROVÓ, A. G. Optimization of fipronil degradation by heterogeneous photocatalysis: Identification of transformation products and toxicity assessment. *Water Research*, v. 110, p. 133–140, 2017.

GUO, W.; LIU, X.; HUO, P.; GAO, X.; WU, D.; LU, Z.; YAN, Y. Hydrothermal synthesis spherical TiO_2 and its photo-degradation property on salicylic acid. *Applied Surface Science*, v. 258, n. 18, p. 6891-6896, 2012.

HAIROM, N.H.H.; MOHAMMAD, A.W.; NG, L.Y.; KADHUM, A.A.H. Utilization of self-synthesized ZnO nanoparticles in MPR for industrial dye wastewater treatment using NF and UF membrane. *Desalination Water Treatment*, v. 54, p. 944–955, 2015.

HANSEN, E.; RODRIGUES, M.A.S.; ARAGÃO, M.E.; AQUIM, P.M. Water and wastewater minimization in a petrochemical industry through mathematical programming. *Journal of Cleaner Production*, v. 172, p. 1814-1822, 2018.

HATAT-FRAILE, M.; LIANG, R.; ARLOS, M. J.; HE, R. X.; PENG, P.; SERVOS, M. R.; ZHOU, Y. Concurrent photocatalytic and filtration processes using doped TiO_2 coated quartz fiber membranes in a photocatalytic membrane reactor. *Chemical Engineering Journal*, v. 330, p. 531–540, 2017.

HO, D. P.; VIGNESWARAN, S.; NGO, H. H. Photocatalysis-membrane hybrid system for organic removal from biologically treated sewage effluent. **S***eparation and Purification Technology*, v. 68, n. 2, p. 145–152, 2009.

HODGES, B.C.; CATES, E.L.; KIM, J. Challenges and prospects of advanced oxidation water treatment processes using catalytic nanomaterials. *Nature Nanotechnology,* v. 13, n. 8, p. 642-650, 2018.

HOLLOWAY, R. W.; REGNERY, J.; NGHIEM, L. D.; CATH, T. Y. Removal of trace organic chemicals and performance of a novel hybrid ultrafiltration-osmotic membrane bioreactor. *Environmental Science and Technology*, v. 48, n. 18, p. 10859–10868, 2014.

IBRAHIM, D. S.; LATHALAKSHMI, M.; MUTHUKRISHNARAJ, A.; BALASUBRAMANIAN, N. An alternative treatment process for upgrade of petroleum refinery wastewater using electrocoagulation. *Petroleum Science*, v. 10, n. 3, p. 421–430, 14 set. 2013.

IGLESIAS, O.; RIVERO, M. J.; URTIAGA, A. M.; ORTIZ, I. Membrane-based photocatalytic systems for process intensification. *Chemical Engineering Journal*, v. 305, p. 136–148, 2016.

IPIECA. Petroleum refining water/wastewater use and management. *Ipieca Operations Best Practice Series*, 2010.

JAMALY, S.; GIWA, A.; HASAN, S. W. Recent improvements in oily wastewater treatment: Progress, challenges, and future opportunities. *Journal of Environmental Sciences (China)*, v. 37, p. 15-30, 2015.

JANSSENS, R.; MANDAL, M. K.; DUBEY, K. K.; LUIS, P. Slurry photocatalytic membrane reactor technology for removal of pharmaceutical compounds from wastewater: Towards cytostatic drug elimination. *Science of the Total Environment*, v. 599, p. 612-626, 2017.

JARUSUTTHIRAK, C.; AMY, G. Role of soluble microbial products (SMP) in membrane fouling and flux decline. *Environmental Science and Technology*, v. 40, n. 3, p. 969–974, 2006.

JING, Y.; LI, L.; ZHANG, Q.; LU, P.; LIU, P.; LÜ, X. Photocatalytic ozonation of dimethyl phthalate with TiO2 prepared by a hydrothermal method. *Journal of hazardous materials,* v. 189, n. 1-2, p. 40-47, 2011.

KAPILASHRAMIM, M.; ZHANG, Y.; LIU, Y.S.; HAGFELDT, A.; GUO, A.J. Probing the optical property and electronic structure of TiO_2 nanomaterials for renewable energy applications. *Chemical Reviews*, v. 114, p. 9662–9707, 2014.

KEIL, F. J.; Process intensification. *Reviews In Chemical Engineering*, v. 34, n. 2, p.135-200, 2018.

KENARI, H.; SARRAFZADEH, M.; TAVAKOLI, O. An investigation on the nitrogen content of a petroleum refinery wastewater and its removal by biological treatment. *Iranian Journal of Environmental Health Science & Engineering*, v. 7, n. 5, p. 391-394, 2010.

KHAN, W.K.; NAJEEB, I.; TUIYEBAYEVA, M.; MAKHTAYEVA, Z. Refinery wastewater degradation with titanium dioxide, zinc oxide, and hydrogen peroxide in a photocatalytic reactor. *Process Safety and Environmental Protection*, v. 94, p. 479-486, 2015.

KIM, Y-H.; PARK, L.K.; YIACOUMI, S.; TSOURIS, C. Modular Chemical Process Intensification: A Review. *Annual Review of Chemical and Biomolecular Engineering*, v. 8, n. 1, p.359-380, 2017.

KOMARNENI, S.; NOH YOUNG, D.; KIM JOO, Y.; KIM SEOK, H.; KATSUKI, H. Solvothermal / hydrothermal synthesis of metal oxides and metal powders with and without microwaves. *Zeitschrift für Naturforschung B,* v. 1033, 2010.

LAI, W.W-P.; LIN, H.H-H; LIN, A.Y-C. TiO_2 photocatalytic degradation and transformation of oxazaphosphorine drugs in an aqueous environment. *Journal of Hazardous Materials*, v. 287, p. 133-141, 2015.

LAWLER, W.; ALVAREZ-GAITAN, J.; LESLIE, G.; LE-CLECH, P. Comparative life cycle assessment of end-of-life options for reverse osmosis membranes. *Desalination*, v. 357, p. 45–54, 2015.

LAWLER, W.; ANTONY, A.; CRAN, M.; DUKE, M.; LESLIE, G.; LE-CLECH, P. Production and characterization of UF membranes by chemical conversion of used RO membranes. *Journal of Membrane Science*, v. 447, p. 203–211, 2013.

LEE, S. A.; CHOO, K. H.; LEE, C. H.; LEE, H. I.; HYEON, T.; CHOI, W.; KWON, H. H. Use of Ultrafiltration Membranes for the Separation of TiO_2 Photocatalysts in Drinking Water Treatment. *Industrial & Engineering Chemistry Research,* v. 40, n. 7, p. 1712–1719, 2002.

LEONG, S., RAZMJOU, A., WANG, K., HAPGOOD, K., ZHANG, X., WANG, H. TiO_2 based photocatalytic membranes: A review**.** *Journal of Membrane Science*, v. 472, p.167-184, 2014.

LI, J. F.; XU, Z. L.; YANG, H.; YU, L. Y.; LIU, M. Effect of TiO_2 nanoparticles on the surface morphology and performance of microporous PES membrane. *Applied Surface Science*, v. 255, n. 9, p. 4725–4732, 2009.

LI, W.; ZENG, T. Preparation of TiO_2 anatase nanocrystals by $TiCl_4$ hydrolysis with additive H_2SO_4. *PLoS ONE,* v. 6, n. 6, p. 1-6, 2011.

LI, X.; WANG, L.; LU, X. Preparation of silver-modified TiO_2 via microwave-assisted method and its photocatalytic activity for toluene degradation. *Journal of Hazardous Materials*, v. 177, n. 1-3, p. 639-647, 2010.

LIANG, S.; LIU, C.; SONG, L. Soluble microbial products in membrane bioreactor operation: Behaviors, characteristics, and fouling potential. *Water Research*, v. 41, n. 1, p. 95-101, 2007.

LING, H.; KIM, K.; LIU, Z.; SHI, J.; ZHU, X.; & HUANG, J. Photocatalytic degradation of phenol in water on as-prepared and surface modified TiO_2 nanoparticles. *Catalysis Today*, v. 258, p. 96-102, 2015.

LINGBO, L.; SONG, Y., CONGBI, H., & GUANGBO, S. Comprehensive characterization of oil refinery effluent-derived humic substances using various spectroscopic approaches. *Chemosphere*, v. 60, n. 4, p. 467-476, 2005.

LIU, P.; ZHANG, H.; FENG, Y.; YANG, F.; ZHANG, J. Removal of trace antibiotics from wastewater: A systematic study of nanofiltration combined with ozone-based advanced oxidation processes. *Chemical Engineering Journal*, v. 240, p. 211–220, 2014.

LOOSLI, F.; LE COUSTUMER, P.; STOLL, S. Impact of alginate concentration on the stability of agglomerates made of TiO_2 engineered nanoparticles: Water hardness and pH effects. *Journal of Nanoparticle Research*, v. 17, n. 1, p. 44, 2015.

LY, Q. V.; HU, Y.; LI, J.; CHO, J.; HUR, J. Characteristics and influencing factors of organic fouling in forward osmosis operation for wastewater applications: A comprehensive review. *Environment International*, v. 129, p. 164-184, 2019.

MA, D.; GAO, B.; SUN, S.; WANG, Y.; YUE, Q.; LI, Q. Effects of dissolved organic matter size fractions on trihalomethanes formation in MBR effluents during chlorine disinfection. *Bioresource Technology*, v. 136, p. 535–541, 2013.

MA, D.; PENG, B.; ZHANG, Y.; GAO, B.; WANG, Y.; YUE, Q.; LI, Q. Influences of dissolved organic matter characteristics on trihalomethanes formation during chlorine disinfection of membrane bioreactor effluents. *Bioresource Technology*, v. 165, n. C, p. 81–87, 2014.

MANFROI, D.C.; DOS ANJOS, A.; CAVALHEIRO, A.A.; PERAZOLLI, L.A.; VARELA, J.A.; ZAGHETE, M.A. Titanate nanotubes produced from microwave-assisted hydrothermal synthesis: Photocatalytic and structural properties. *Ceramics International*, v. 40, p. 14483-14491, 2014.

MARTINI, S.; ANG, H.M.; ZNAD, H. Integrated Ultrafiltration Membrane Unit for Efficient Petroleum Refinery Effluent Treatment. *Clean - Soil, Air, Water*, v. 45, n. 2, p. 342-353, 2017.

MATSUMOTO, H.; KAKIBAYASHI, H.; TANIGUCHI, Y.; CHENG, I-K; LEE, T-T.; HU, C-L.; LEE, C-T.; FUJIMOTO, M. Characterization of solid-state reaction of barium carbonate and titanium dioxide by spatially resolved electron energy loss spectroscopy. *Journal of the American Ceramic Society*, v. 96, n. 8, p. 2651-2656, 2013.

MENG, F.; ZHANG, S.; OH, Y.; ZHOU, Z.; SHIN, H. S.; CHAE, S. R. Fouling in membrane bioreactors: An updated review**.** *Water Research***,** v. 114, p. 151-180, 2017.

MESQUITA, P. D. L.; SOUZA, C. R.; SANTOS, N. T. G.; ROCHA, S. D. F. Fixed-bed study for bone char adsorptive removal of refractory organics from electrodialysis concentrate produced by petroleum refinery. *Environmental Technology (United Kingdom)*, v. 39, n. 12, p. 1544–1556, 2018.

MIRZAEI, A.; NERI, G. Microwave-assisted synthesis of metal oxide nanostructures for gas sensing application: a review. *Sensors Actuators B Chemical*, v. 237, p. 749–775, 2016.

MOHADESI, A.; RANJBAR, M. Synthesis and characterization of TiO_2 nanoparticles by microwave method and investigation its photovoltaic property. *Journal of Materials Science: Materials in Electronics,* v. 27, n.1, p. 862-866, 2015.

MOHAMED, M.A.; SALLEH, W.N.W.; JAAFAR, J.; ROSMI, M.S.; HIR, Z.A.M.; MUTALIB, M.A.; TANEMURA, M. Carbon as amorphous shell and interstitial dopant in mesoporous rutile TiO2: Bio-template assisted sol-gel synthesis and photocatalytic activity. *Applied Surface Science*, v. 393, p. 46-59, 2017.

MOHD HIR, Z.A.; ALI, R.; WAN ABU BAKAR, W.A. Photodegradation of benzene–toluene–xylene in petroleum refinery waste water by $ZnO/SnO_2/WO_3$ and $ZnO/TiO_2/WO_3$ ternary photocatalysts. *UMTAS*, p. 54–61, 2011.

MOLINARI, R.; LAVORATO, C.; ARGURIO, P. Recent progress of photocatalytic membrane reactors in water treatment and in synthesis of organic compounds. A review. *Catalysis Today*, v. 281, p. 144–164, 2017.

MOSER, P. B.; RICCI, B. C.; REIS, B. G.; NETA, L. S.; CERQUEIRA, A. C.; AMARAL, M. C. Effect of MBR-H_2O_2/UV Hybrid pre-treatment on nanofiltration performance for the treatment of petroleum refinery wastewater. *Separation and Purification Technology*, v. 192, p. 176–184, 2018.

MOSER, P.B.; BRETAS, C.; PAULA, E. C.; FARIA, C.; RICCI, B. C.; CERQUEIRA, A.C.F.;

AMARAL, M.C.S. Comparison of hybrid ultrafiltration-osmotic membrane bioreactor and conventional membrane bioreactor for oil refinery effluent treatment. *Chemical Engineering Journal*, v. 378, p. 52-60, 2019.

MOSER, P.B.; RICCI, B.C.; ALVIM, C.B.; CERQUEIRA, A.C.F.; AMARAL, M.C.S. Removal of organic matter of electrodialysis reversal brine from a petroleum refinery wastewater reclamation plant by UV and UV/H_2O_2 process, *Journal of Environmental Science and Health, Part A,* v. 53, n. 5, p. 430-435, 2017.

MOSLEHYANI, A.; ISMAIL, A. F.; OTHMAN, M. H. D.; MATSUURA, T. Design and performance study of hybrid photocatalytic reactor-PVDF/MWCNT nanocomposite membrane system for treatment of petroleum refinery wastewater. *Desalination*, v. 363, p. 99–111, 2015.

MOZIA, S. Photocatalytic membrane reactors (PMRs) in water and wastewater treatment. A review. *Separation and Purification Technology,* v. 73, n. 2, p. 71-91, 2010.

MOZIA, S.; SZYMAŃSKI, K.; MICHALKIEWICZ, B.; TRYBA, B.; TOYODA, M., MORAWSKI, A. W. Effect of process parameters on fouling and stability of MF/UF TiO_2 membranes in a photocatalytic membrane reactor. *Separation and Purification Technology,* v. 142, p. 137–148, 2015.

MUROV, S.L. Handbook of Photochemistry, Marcel Dekker, New York, 1973.

NASSEH, N.; TAGHAVI, L.; BARIKBIN, B.; NASSERI, M.A. Synthesis and characterizations of a novel $FeNi_3/SiO_2/CuS$ magnetic nanocomposite for photocatalytic degradation of tetracycline in simulated wastewater. *Journal of Cleaner Production*, v. 179, p. 42-54, 2018.

NEOH, C. H.; NOOR, Z. Z.; MUTAMIM, N. S. A.; LIM, C. K. Green technology in wastewater treatment technologies: Integration of membrane bioreactor with various wastewater treatment systems. *Chemical Engineering Journal*, v. 283, p.582-594, 2016.

NIU, J.; YAO, B.; PENG, C.; ZHANG, W.; CHEN, Y. Rapid Microwave Hydrothermal Methods Synthesis of TiO_2 Photocatalysts Using Different Sources of Materials. *Integrated Ferroelectrics*, v. 152, n. 1, p. 163-173, 2014.

NOGUEIRA, A. A.; BASSIN, J. P.; CERQUEIRA, A. C.; DEZOTTI, M. Integration of biofiltration and advanced oxidation processes for tertiary treatment of an oil refinery wastewater aiming at water reuse. *Environmental Science and Pollution Research*, v. 23, n. 10, p. 9730–9741, 2016.

NOMAN, M. T.; ASHRAF, M. A.; ALI, A. Synthesis and applications of nano-TiO_2: a review. *Environmental Science and Pollution Research***,** v. 26, n. 4, p. 3262-3291, 2018.

ONG, C.B.; MOHAMMAD, A.W.; NG, L.Y. Integrated adsorption-solar photocatalytic membrane reactor for degradation of hazardous Congo red using Fe-doped ZnO and Fe-doped ZnO/rGO nanocomposites. *Environmental Science and Pollution Research*, p.1-14, 2018.

OSIN, O.; YU, T.; CAI, X.; JIANG, Y.; PENG, G.; CHENG, X.; LIN, S. Photocatalytic degradation of 4-nitrophenol by C, N-TiO_2: Degradation efficiency vs. embryonic toxicity of the resulting compounds. *Frontiers in chemistry*, v. 6, p. 192, 2018.

PADAKI, M.; MURALI, R. S.; ABDULLAH, M. S.; MISDAN, N.; MOSLEHYANI, A.; KASSIM, M. A.; ISMAIL, A. F. Membrane technology enhancement in oil-water separation. A review. *Desalination*, v. 357, p. 197-207, 2015.

PAKRAVAN, P.; AKHBARI, A.; MORADI, H.; AZANDARYANI, A.; MANSOURI, A.; SAFARI, M. Process modeling and evaluation of petroleum refinery wastewater treatment through response surface methodology and artificial neural network in a photocatalytic reactor using poly ethyleneimine (PEI)/titania (TiO_2) multilayer film on quartz tube. *Applied Petrochemical Research*, v. 5, n. 1, p. 47-59, 2014.

PATIL, S. R.; AKPAN, U. G.; HAMEED, B. H.; SAMDARSHI, S. K. A comparative study of the photocatalytic efficiency of Degussa P25, Qualigens, and Hombikat UV-100 in the degradation kinetic of congo red dye. *Desalination and Water Treatment*, v. 46, n. 1-3, p. 188-195, 2012.

PAULA, E.C.; GOMES, J.C.L.; AMARAL, M.C.S. Recycling of end-of-life reverse osmosis membranes by oxidative treatment: a technical evaluation. *Water Science and Technology*, v. 76, n. 3, p. 605-622, 2017.

PENDASHTEH, A. R.; FAKHRU'L-RAZI, A.; MADAENI, S. S.; ABDULLAH, L. C.; ABIDIN, Z. Z.;BIAK, D. R. A. Membrane foulants characterization in a membrane bioreactor (MBR) treating hypersaline oily wastewater. *Chemical Engineering Journal,* v. 168, n. 1, p. 140–150, 2011.

PETROBRÁS, Recursos Hídricos, 2018. <Disponível em: http://www.petrobras.com.br/pt/sociedade-e-meio-ambiente/meio-ambiente/recursos-hidricos/> acessado dia 12 de outubro de 2018

PLAKAS, K. V.; SARASIDIS, V. C.; PATSIOS, S. I.; LAMBROPOULOU, D. A.; KARABELAS, A. J. Novel pilot scale continuous photocatalytic membrane reactor for removal of organic micropollutants from water. *Chemical Engineering Journal*, v. 304, p. 335–343, 2016.

RAMESH, A.; LEE, D. J.; HONG, S. G. Soluble microbial products (SMP) and soluble extracellular polymeric substances (EPS) from wastewater sludge. *Applied Microbiology and Biotechnology*, v. 73, n. 1, p. 219–225, 2006.

RAZMJOU, A.; MANSOURI, J.; CHEN, V. The effects of mechanical and chemical modification of TiO2 nanoparticles on the surface chemistry, structure and fouling performance of PES ultrafiltration membranes. *Journal of Membrane Science*, v. 378, n. 1–2, p. 73–84, 2011.

REINKE, M.; PONOMAREV, E.; KUZMINYKH, Y.; HOFFMANN, P. Combinatorial Characterization of TiO_2 Chemical Vapor Deposition Utilizing Titanium Isopropoxide. *Acs Combinatorial Science*, v. 17, n. 7, p. 413-420, 2015.

RUEDA-MÁRQUEZ, J. J.; LEVCHUK, I.; SALCEDO, I.; ACEVEDO-MERINO, A.; MANZANO, M.A. Post-treatment of refinery wastewater effluent using a combination of AOPs (H_2O_2 photolysis and catalytic wet peroxide oxidation) for possible water reuse. Comparison of low and medium pressure lamp performance. *Water Research*, v. 91, p. 86-96, 2016.

SAIEN, J.; NEJATI, H. Enhanced photocatalytic degradation of pollutants in petroleum refinery wastewater under mild conditions. *Journal of hazardous materials*, v. 148, n. 1-2, p. 491-495, 2007.

SHAHREZAEI, F.; MANSOURI, Y.; ZINATIZADEH, A.A.L.; AKHBARI, A. Process modeling and kinetic evaluation of petroleum refinery wastewater treatment in a photocatalytic reactor using TiO_2 nanoparticles. *Powder Technology*, v. 221, p. 203-212, 2012.

SHEN, P.S.; TAI, Y.C.; CHEN, P.; WU, Y.C. Clean and time-effective synthesis of anatase TiO_2 nanocrystalline by microwave assisted solvothermal method for dye-sensitized solar cells. *Journal of Power Sources*, v. 247, p. 444-451, 2014.

SHENVI, S.S.; ISLOOR, A.M.; ISMAIL, A.F. A review on RO membrane technology: Developments and challenges. *Desalination*, v. 368, p. 10–26, 2015.

SOUZA, B. M.; CERQUEIRA, A. C.; SANT'ANNA, G.L.; DEZOTTI, M. Oil-refinery wastewater treatment aiming reuse by advanced oxidation processes (AOPs) combined with biological activated carbon (BAC). *Ozone: Science & Engineering*, v. 33, n. 5, p. 403-409, 2011.

SOUZA, B. M.; SOUZA, B. S.; GUIMARÃES, T. M.; RIBEIRO, T. F.; CERQUEIRA, A. C.; SANT'ANNA, G. L.; DEZOTTI, M. Removal of recalcitrant organic matter content in wastewater by means of AOPs aiming industrial water reuse. *Environmental Science and Pollution Research*, v. 23, n. 22, p. 22947–22956, 2016.

SPASIANO, D.; SICILIANO, A.; RACE, M.; MAROTTA, R.; GUIDA, M.; ANDREOZZI, R.; PIROZZI, F. Biodegradation, ecotoxicity and UV_{254}/H_2O_2 treatment of imidazole, 1-methyl-imidazole and N,N'-alkyl-imidazolium chlorides in water. *Water Research*, v. 106, p. 450–460, 2016.

SZYMAŃSKI, K.; MORAWSKI, A.W.; MOZIA, S. Effectiveness of treatment of secondary effluent from a municipal wastewater treatment plant in a photocatalytic membrane reactor and hybrid UV/H_2O_2 – ultrafiltration system. *Chemical Engineering and Processing - Process Intensification*, v. 125, p. 318-324, 2018.

TIAN, Y.; LU, Y.; LI, Z. Performance analysis of a combined system of membrane bioreactor and worm reactor: wastewater treatment, sludge reduction and membrane fouling. *Bioresource technology*, v. 121, p. 176-182, 2012.

TOPARE, N.S.; JOY, M.; JOSHI, R.R.; JADHAV, P.B.; KASHIRSAGAR, L.K. Treatment of petroleum industry wastewater using TiO_2/UV photocatalytic process. *Journal of Indian Chemical Society*, v. 92, p. 219-222, 2015.

VAIANO, V.; SACCO, O.; SANNINO, D.; CIAMBELLI, P. Process intensification in the removal of organic pollutants from wastewater using innovative photocatalysts obtained coupling Zinc Sulfide based phosphors with nitrogen doped semiconductors. *Journal of Cleaner Production*, v. 100, p. 208-211, 2015.

VAN GERVEN, T.; STANKIEWICZ, A. Structure, Energy, Synergy, Time: The Fundamentals of Process Intensification. *Industrial & Engineering Chemistry Research*, v. 48, n. 5, p. 2465-2474, 2009.

VELA, M. C. V., BLANCO, S. Á., GARCÍA, J. L., & RODRÍGUEZ, E. B. Analysis of membrane pore blocking models applied to the ultrafiltration of PEG. *Separation and Purification Technology*, v. 62, n. 3, p. 489–498, 2008.

VENDRAMEL, S.; BASSIN, J.P.; DEZOTTI, M.; SANT' ANNA JR, G.L. Treatment of petroleum refinery wastewater containing heavily polluting substances in an aerobic submerged fixed-bed reactor, *Environmental. Technology*, v. 36, 2052-205, 2015.

VENZKE, C.D.; GIACOBBO, A.; KLAUCK, C.R.; VIEGAS, C.; HANSEN, E.; MONTEIRO DE AQUIM, P.; BERNARDES, A.M. Integrated Membrane Processes (EDR-RO) for Water Reuse in the Petrochemical Industry. *Journal Of Membrane Science And Research*, v. 4, n. 4, p. 218-226, 2018.

VIANA, M.M.; SOARES, V.F.; MOHALLEM, N.D.S. Synthesis and characterization of TiO_2 nanoparticles. *Ceramics International*, v. 36, n. 7, p. 2047-2053, 2010.

WAKE, H. Oil refineries: a review of their ecological impacts on the aquatic environment. *Estuarine, Coastal and Shelf Science*, v. 62, n. 1-2, p. 131–140, 2005.

WANG, H.; MUSTAFFAR, A.; PHAN, A.N.; ZIVKOVIC, V.; REAY, D.; LAW, R.; BOODHOO, K. A review of process intensification applied to solids handling. *Chemical Engineering And Processing: Process Intensification*, v. 118, p.78-107, 2017.

WANG, X.J.; LI, F.T.; LIU, J.X.; KOU, C.G.; ZHAO, Y.; HAO, Y.J.; ZHAO, D. Preparation of TiO_2 in ionic liquid via microwave radiation and in situ photocatalytic oxidative desulfurization of diesel oil. *Energy & Fuels,* v. 26, n. 11, p. 6777-6782, 2012.

WANG, Z. B.; GUAN, Y. J.; CHEN, B.; BAI, S. L. Retention and separation of 4BS dye from wastewater by the N-TiO_2 ceramic membrane. *Desalination and Water Treatment*, v. 57, n. 36, p. 16963–16969, 2016.

YE, Y.; BRUNING, H.; LI, X.; YNTEMA, D.; RIJNAARTS, H.H.M. Significant enhancement of micropollutant photocatalytic degradation using a TiO_2 nanotube array photoanode based photocatalytic fuel cell. *Chemical Engineering Journal*, v. 354, p. 553-562, 2018.

ZHANG, P.; YIN, S.; SATO, T. Synthesis of high-activity TiO_2 photocatalyst via environmentally friendly and novel microwave assisted hydrothermal process. *Applied Catalysis B,* v. 89, p. 118–122, 2009.

ZHANG, X.; LI, D.; WAN, J.; YU, X. Hydrothermal synthesis of TiO_2 nanosheets photoelectrocatalyst on Ti mesh for degradation of norfloxacin: Influence of pickling agents. *Materials Science in Semiconductor Processing*, v. 43, p. 47-54, 2016.

ZHANG, G.; ZHANG, J.; WANG, L.; MENG, Q.; WANG, J. Fouling mechanism of low-pressure hollow fiber membranes used in separating nanosized photocatalysts. *Journal of Membrane Science*, v. 389, p. 532–543, 2012.

ZHANG, W.; DING, L.; LUO, J.; JAFFRIN, M. Y.; TANG, B. Membrane fouling in photocatalytic membrane reactors (PMRs) for water and wastewater treatment: A critical review**.** *Chemical Engineering Journal,* 2016.

ZHANG, Y.; WEI, S.; HU, Y.; SUN, S. Membrane technology in wastewater treatment enhanced by functional nanomaterials. *Journal of Cleaner Production,* v. 197, p. 339–348, 2018.

ZHAO, C.; GU, P.; ZHANG, G. A hybrid process of powdered activated carbon countercurrent two-stage adsorption and microfiltration for petrochemical RO concentrate treatment. *Desalination*, v. 330, p. 9-15, 2013.

ZHOU, C., YE, D., JIA, H., YU, S., LIU, M., & GAO, C. Surface mineralization of commercial thin-film composite polyamide membrane by depositing barium sulfate for improved reverse osmosis performance and antifouling property. *Desalination,* v. 351, p. 228–235, 2014.

ZIOLKOWSKA, J. R. Is Desalination Affordable?—Regional Cost and Price Analysis**.** *Water Resources Management,* v. 29, n. 5, p. 1385-1397, 2015.

ZUBIETA, C.E.; SOLTERO-MARTÍNEZ, J.F.A.; LUENGO, C.V.; SCHULZ, P.C. Preparation, characterization and photoactivity of TiO_2 obtained by a reverse microemulsion route. *Powder Technology*, v. 212, p. 410–417, 2011.